ELSEVIER

Comput. Methods Appl. Mech. Engrg. 191 (2002) 1129–1157

Computer methods in applied mechanics and engineering

www.elsevier.com/locate/cma

A numerical scheme to couple subdomains with different time-steps for predominantly linear transient analysis

Alain Combescure *, Anthony Gravouil

LMT/ENS Cachan/CNRS, 61 avenue du président Wilson, 94235 Cachan Cedex, France

Received 15 December 1998; received in revised form 26 April 2000

Abstract

This paper generalizes the explicit/implicit time-integration algorithms pioneered by Belytschko, Hughes and their respective co-workers, and the FETI domain decomposition methods introduced by Farhat and his co-workers, to the case where the same Newmark scheme, but different β and γ coefficients and different time-steps, are specified in each subdomain. Building upon the work of Farhat, Crivelli and Géradin, it considers various interface boundary constraints and performs a stability analysis of the proposed time integration algorithms.

0. Introduction

Today, nonlinear dynamic calculations can be classified into different timescale families: first, crash and perforation problems with short timescales; next, seismic problems with long time periods; finally, impact-generated vibrations which require two timescales [1,2]. For example, an impact on the containment vessel of a nuclear power plant reactor leads to timescales on the order of a hundredth of a second, whereas the subsequent shaking of the structure leads to vibrations on the order of 1 s [3]. In the last case, it is possible to distinguish between the impact zone, whose behavior is nonlinear, and the rest of the structure [4,5]. Thus, it turns out that the time and space scales of phenomena are different for these two domains. Therefore, we are confronted with both a fast dynamics problem and a dynamic vibration problem. We propose to implement a time integration method which allows the coupling of the classical methods adapted to each phenomenon. The first step is to partition the domain into subdomains using a dual Schur discretized formulation [6]. Then, we consider the Newmark scheme with the intention of coupling explicit and/or implicit numerical schemes for the time integration [7–10]. Next, we propose to use an energy formulation [11] to prove that the numerical stability of the global problem depends on continuity conditions prescribed at the interface. For the discretized problem, we can prescribe displacement, velocity or

* Corresponding author. Tel.: +33-14-740-2832; fax: +33-14-740-2785.
E-mail addresses: combescure@lmt.ens-cachan.fr (A. Combescure), gravouil@lmt.ens-cachan.fr (A. Gravouil).

0045-7825/02/$ - see front matter
PII: S0045-7825(01)00190-6

acceleration continuity at the interface. This study shows that a continuity constraint on velocities at the interface is the best choice to couple subdomains with different time-steps and different Newmark numerical schemes. Then, we propose an extension to the nonlinear case for explicit subdomains with fixed time-steps. Finally, we validate the method and study its advantages and limitations through three examples.

1. Implementation of the method

1.1. Dynamics formulation of the reference problem

The aim of this work is to present a method which allows to couple time integration algorithms of the Newmark family in a finite element context. We are concerned with the motion, in the time interval $[0, T]$, of a deformable solid occupying a domain Ω. The action functional for the solid is

$$L(\mathbf{U}, \dot{\mathbf{U}}) = \int_0^T \left[\frac{1}{2} \dot{\mathbf{U}}^{\mathrm{T}} \mathbf{M} \dot{\mathbf{U}} - \Phi(\mathbf{U}) + \mathbf{F}_{\mathrm{ext}}^{\mathrm{T}} \mathbf{U} \right] \mathrm{d}t, \tag{1.1}$$

where $\mathbf{U}$ and $\dot{\mathbf{U}}$ represent the displacement and velocity vectors, $\mathbf{M}$ the symmetric, positive definite mass matrix, Φ designates the strain energy and $\mathbf{F}_{\mathrm{ext}}$ the externally applied forces. The equations of motion of the spatially discretized solid follow from the requirement that L be stationary:

$$\mathbf{M}\ddot{\mathbf{U}} + \mathbf{F}_{\mathrm{int}}(\mathbf{U}) = \mathbf{F}_{\mathrm{ext}}, \tag{1.2}$$

where $\mathbf{F}_{\mathrm{int}}(\mathbf{U})$ are the internal forces and $\ddot{\mathbf{U}}$ the acceleration vector. Eq. (1.2) in conjunction with initial conditions of the form

$$\begin{aligned} &\mathbf{U}(0) = \mathbf{U_0}, \\ &\dot{\mathbf{U}}(0) = \dot{\mathbf{U}}_{\mathbf{0}} \end{aligned} \tag{1.3}$$

defines an initial value problem to be solved for $\mathbf{U}$ and $\dot{\mathbf{U}}$.

Then, we partition the structure Ω into s subdomains using a dual Schur formulation of functional (1.1) [12–14]:

$$L = \sum_{k=1}^{s} L_k + L_{\mathrm{link}}, \tag{1.4}$$

where we assume that the interface energy is obtained, for example, from the definition of linear link equations:

$$L_{\mathrm{link}} = \int_0^T \lambda^{\mathrm{T}} \mathbf{C}\mathbf{W} \, \mathrm{d}t \quad \text{with } \mathbf{C}\mathbf{W} = \sum_{k=1}^{s} \mathbf{C}^k \mathbf{W}^k = \sum_{k=1}^{s} \sum_{i=1}^{l} \mathbf{C}_i^k \mathbf{W}^k, \tag{1.5}$$

where l is the number of interfaces, λ the column vector of Lagrange multipliers and $\mathbf{C}$ the constraint matrix which connects all subdomains together; $\mathbf{W}$ is the displacement, velocity or acceleration vector, depending on the choice of the kinematic interface constraints. If we consider only matching interfaces, the constraint matrix is Boolean. The significance of the Lagrange multiplier λ depends on the choice of constraints, but the global functional is the same. The reference equations are then obtained by requiring that functional (1.4) be stationary:

$$\begin{aligned} &\mathbf{M}^k \ddot{\mathbf{U}}^k + \mathbf{F}_{\mathrm{int}}^k = \mathbf{F}_{\mathrm{ext}}^k + \mathbf{F}_{\mathrm{link}}^k \quad \forall k \in \{1, \ldots, s\}, \\ &\textstyle\sum_{k=1}^{s} \mathbf{C}^k \mathbf{W}^k = 0, \end{aligned} \quad \text{with } \mathbf{F}_{\mathrm{link}}^k = \mathbf{C}^{k^{\mathrm{T}}} \Lambda, \tag{1.6}$$

where Λ represents the undetermined interface "loads" between the subdomains [15]. We can observe in Eq. (1.6) that the acceleration vector $\ddot{\mathbf{U}}^k$ is the sum of two terms: an acceleration $\ddot{\mathbf{U}}^k_{\text{free}}$ obtained from internal and external loads alone and an acceleration $\ddot{\mathbf{U}}^k_{\text{link}}$ obtained from the link loads. Consequently, we can uncouple the equilibrium equation on each subdomain into a "free problem" and a "link problem":

$$\begin{aligned}
&\mathbf{M}^k\ddot{\mathbf{U}}^k_{\text{free}} + \mathbf{F}^k_{\text{int}} = \mathbf{F}^k_{\text{ext}} \quad \forall k \in \{1,\dots,s\},\\
&\mathbf{M}^k\ddot{\mathbf{U}}^k_{\text{link}} = \mathbf{F}^k_{\text{link}} \quad \forall k \in \{1,\dots,s\},\\
&\ddot{\mathbf{U}}^k = \ddot{\mathbf{U}}^k_{\text{free}} + \ddot{\mathbf{U}}^k_{\text{link}} \quad \forall k \in \{1,\dots,s\},\\
&\textstyle\sum_{k=1}^{s} \mathbf{C}^k\mathbf{W}^k = 0.
\end{aligned} \tag{1.7}$$

In order to present the basic algorithm, we make the following assumptions:

- The time discretization is the same for each subdomain.
- The acceleration is continuous at the interface.
- The internal loads do not depend on the link parameters.

We can then solve problem (1.7) for each time-step $t \in [0,T]$ using the following algorithm:

(a) Solve the free problem on each subdomain:

$$\mathbf{M}^k\ddot{\mathbf{U}}^k_{\text{free}} + \mathbf{F}^k_{\text{int}} = \mathbf{F}^k_{\text{ext}} \quad \forall k \in \{1,\dots,s\}. \tag{1.8}$$

(b) Calculate the Lagrange multipliers Λ using the condensed global problem:

$$\mathbf{C}\ddot{\mathbf{U}} = 0 \iff \mathbf{C}\ddot{\mathbf{U}}_{\text{link}} = -\mathbf{C}\ddot{\mathbf{U}}_{\text{free}} \iff \mathbf{H}\Lambda = -\mathbf{C}\ddot{\mathbf{U}}_{\text{free}} \quad \text{with } \mathbf{H} = \sum_{k=1}^{s} \mathbf{C}^k\mathbf{M}^{k^{-1}}\mathbf{C}^{k^{\mathrm{T}}}. \tag{1.9}$$

(c) Solve the link problem on each subdomain:

$$\mathbf{M}^k\ddot{\mathbf{U}}^k_{\text{link}} = \mathbf{C}^{k^{\mathrm{T}}}\Lambda \quad \forall k \in \{1,\dots,s\}. \tag{1.10}$$

(d) Calculate the acceleration for the global problem:

$$\ddot{\mathbf{U}}^k = \ddot{\mathbf{U}}^k_{\text{free}} + \ddot{\mathbf{U}}^k_{\text{link}} \quad \forall k \in \{1,\dots,s\}. \tag{1.11}$$

Remark.

- This algorithm is the basis for the different methods developed in this paper: for example, with the same or different time-steps on all subdomains, as well as in the linear or the nonlinear case.
- For the transient problem studied there, the $\mathbf{H}$ matrix can always be determined because $\mathbf{M}^k$ is not singular and we do not need to take into account the rigid modes of the floating subdomains [16].
- This approach is particularly appropriate for parallel computers; for example, Eqs. (1.8), (1.10) and (1.11) can be solved in a parallel way in each subdomain.
- There is a important difference between the discretized formulation and the continuous formulation: in the continuous case, displacements, velocities and accelerations are continuous at the interfaces.

However, from a numerical point of view, only one of these quantities can be prescribed at the interfaces. Therefore, we will address the different cases separately.

1.2. Approximate solution in time

Each subdomain k is discretized in time with its own Newmark numerical scheme [17,18] characterized by the two parameters β_k and γ_k. Then we can choose an explicit or an implicit scheme for each subdomain. Next, we want to compute kinematic quantities at time t_{n+1} from the known quantities at time t_n. For each subdomain, we can write

$$\begin{aligned}
&\mathbf{U}^k_{n+1} = \mathbf{U}^k_n + \Delta t_k \dot{\mathbf{U}}^k_n + \Delta t_k^2 \left(\tfrac{1}{2} - \beta_k\right) \ddot{\mathbf{U}}^k_n + \Delta t_k^2 \beta_k \ddot{\mathbf{U}}^k_{n+1}, \\
&\dot{\mathbf{U}}^k_{n+1} = \dot{\mathbf{U}}^k_n + \Delta t_k (1 - \gamma_k) \ddot{\mathbf{U}}^k_n + \Delta t_k \gamma_k \ddot{\mathbf{U}}^k_{n+1},
\end{aligned} \quad \text{with } t^k_{n+1} = t^k_n + \Delta t_k. \tag{1.12}$$

From the values at the beginning of the time-step (index n), we introduce the predictors ${}^{\mathrm{p}}\mathbf{U}^k_n$ and ${}^{\mathrm{p}}\dot{\mathbf{U}}^k_n$ given by

$$\begin{aligned}
&{}^{\mathrm{p}}\mathbf{U}^k_n = \mathbf{U}^k_n + \Delta t_k \dot{\mathbf{U}}^k_n + \Delta t_k^2 \left(\tfrac{1}{2} - \beta_k\right) \ddot{\mathbf{U}}^k_n, \\
&{}^{\mathrm{p}}\dot{\mathbf{U}}^k_n = \dot{\mathbf{U}}^k_n + \Delta t_k (1 - \gamma_k) \ddot{\mathbf{U}}^k_n.
\end{aligned} \tag{1.13}$$

We will, from now on, omit the time-step symbol n or $n+1$ except where it is absolutely necessary, with the understanding that unknown quantities are always associated with time t_{n+1} and known quantities with time t_n (except for externally applied forces)

$$\begin{aligned}
&\mathbf{U}^k = {}^{\mathrm{p}}\mathbf{U}^k + \Delta t_k^2 \beta_k \ddot{\mathbf{U}}^k, \\
&\dot{\mathbf{U}}^k = {}^{\mathrm{p}}\dot{\mathbf{U}}^k + \Delta t_k \gamma_k \ddot{\mathbf{U}}^k.
\end{aligned} \tag{1.14}$$

2. Coupling between different numerical schemes in time

In this section we will show how we can achieve the coupling between subdomains each with its own time-step and Newmark scheme. In order to express kinematic continuity at the interfaces in a general way (see (1.6)), we now introduce the following notations:

$$\begin{aligned}
&\alpha^k_1 = 1 && \mathbf{W}^k_1 = \ddot{\mathbf{U}}^k \\
&\alpha^k_2 = \gamma_k \Delta t_k \quad \text{and} && \mathbf{W}^k_2 = \dot{\mathbf{U}}^k \\
&\alpha^k_3 = \beta_k \Delta t_k^2 && \mathbf{W}^k_3 = \mathbf{U}^k,
\end{aligned} \tag{2.1}$$

where $\mathbf{W}^k_1, \mathbf{W}^k_2$ and $\mathbf{W}^k_3$ correspond, respectively, to acceleration, velocity or displacement continuity at the interface between subdomains. Then, we can write $\mathbf{W}^k_z$ in the form:

$$\mathbf{W}^k_z = {}^{\mathrm{p}}\mathbf{W}^k_z + \alpha^k_z \ddot{\mathbf{U}}^k, \quad z \in \{1,2,3\} \tag{2.2}$$

with

$$\begin{aligned}
&{}^{\mathrm{p}}\mathbf{W}^k_1 = 0, \\
&{}^{\mathrm{p}}\mathbf{W}^k_2 = {}^{\mathrm{p}}\dot{\mathbf{U}}^k, \\
&{}^{\mathrm{p}}\mathbf{W}^k_3 = {}^{\mathrm{p}}\mathbf{U}^k.
\end{aligned} \tag{2.3}$$

2.1. Identical time-steps in all subdomains

We will now address the resolution of discretized problem (1.6) using Eqs. (1.12) and (1.13) in the special case, where

$$\Delta t_k = \Delta t \quad \forall k \in \{1, \ldots, s\}. \tag{2.4}$$

In order to simplify the presentation, we will assume that the behavior is elastic. Therefore

$$\mathbf{F}^k_{\mathrm{int}} = \mathbf{K}^k \mathbf{U}^k, \tag{2.5}$$

where $\mathbf{K}^k$ represents the stiffness matrix of subdomain k.

Then, if we substitute expressions (1.12) and (2.2) in Eq. (1.6), we can write it in the following matrix form:

$$\begin{pmatrix} \alpha_z^1\tilde{\mathbf{M}}^1 & 0 & 0 & -\alpha_z^1\mathbf{C}^{1\mathrm{T}} \\ 0 & \cdots & 0 & \cdots \\ 0 & 0 & \alpha_z^s\tilde{\mathbf{M}}^s & -\alpha_z^s\mathbf{C}^{s\mathrm{T}} \\ -\alpha_z^1\mathbf{C}^1 & \cdots & -\alpha_z^s\mathbf{C}^s & 0 \end{pmatrix} \begin{pmatrix} \ddot{\mathbf{U}}^1 \\ \vdots \\ \ddot{\mathbf{U}}^s \\ \Lambda \end{pmatrix} = \begin{pmatrix} \alpha_z^1\left(\mathbf{F}_{\mathrm{ext}}^1 - \mathbf{K}^1\,{}^{\mathrm{p}}\mathbf{U}^1\right) \\ \vdots \\ \alpha_z^s\left(\mathbf{F}_{\mathrm{ext}}^s - \mathbf{K}^s\,{}^{\mathrm{p}}\mathbf{U}^s\right) \\ \sum_{k=1}^s \mathbf{C}^k\,{}^{\mathrm{p}}\mathbf{W}_z^k \end{pmatrix} \tag{2.6}$$

with

$$\tilde{\mathbf{M}}^k = \mathbf{M}^k + \alpha_3^k\mathbf{K}^k. \tag{2.7}$$

As in Section 1.1, we will subdivide Eqs. (2.6) and (2.2) into a free problem:

$$\begin{pmatrix} \tilde{\mathbf{M}}^1 & 0 & 0 & 0 \\ 0 & \cdots & 0 & \cdots \\ 0 & 0 & \tilde{\mathbf{M}}^s & 0 \\ 0 & \cdots & 0 & 0 \end{pmatrix} \begin{pmatrix} \ddot{\mathbf{U}}_{\mathrm{free}}^1 \\ \vdots \\ \ddot{\mathbf{U}}_{\mathrm{free}}^s \\ 0 \end{pmatrix} = \begin{pmatrix} \mathbf{F}_{\mathrm{ext}}^1 - \mathbf{K}^1\,{}^{\mathrm{p}}\mathbf{U}^1 \\ \vdots \\ \mathbf{F}_{\mathrm{ext}}^s - \mathbf{K}^s\,{}^{\mathrm{p}}\mathbf{U}^s \\ 0 \end{pmatrix} \tag{2.8}$$

with

$$\mathbf{W}_{z_{\mathrm{free}}}^k = {}^{\mathrm{p}}\mathbf{W}_z^k + \alpha_z\ddot{\mathbf{U}}_{\mathrm{free}}^k \tag{2.9}$$

and a link problem

$$\begin{pmatrix} \alpha_z^1\tilde{\mathbf{M}}^1 & 0 & 0 & -\alpha_z^1\mathbf{C}^{1\mathrm{T}} \\ 0 & \cdots & 0 & \cdots \\ 0 & 0 & \alpha_z^s\tilde{\mathbf{M}}^s & -\alpha_z^s\mathbf{C}^{s\mathrm{T}} \\ -\alpha_z^1\mathbf{C}^1 & \cdots & -\alpha_z^s\mathbf{C}^s & 0 \end{pmatrix} \begin{pmatrix} \ddot{\mathbf{U}}_{\mathrm{link}}^1 \\ \vdots \\ \ddot{\mathbf{U}}_{\mathrm{link}}^s \\ \Lambda \end{pmatrix} = \begin{pmatrix} 0 \\ \vdots \\ 0 \\ \sum_{k=1}^s \mathbf{C}^k\,{}^{\mathrm{p}}\mathbf{W}_z^s + \sum_{k=1}^s \alpha_z^k\mathbf{C}^k\ddot{\mathbf{U}}_{\mathrm{free}}^k \end{pmatrix} \tag{2.10}$$

with

$$\mathbf{W}_{z_{\mathrm{link}}}^k = \alpha_z\ddot{\mathbf{U}}_{\mathrm{link}}^k. \tag{2.11}$$

Eq. (2.8) corresponds to the solution of the equations of movement in each subdomain independently. Eq. (2.10) corresponds to a correction of the preceding quantities using the constraint loads. The latter problem can be condensed on the interfaces:

$$\begin{pmatrix} \alpha_z^1\tilde{\mathbf{M}}^1 & 0 & 0 & -\alpha_z^1\mathbf{C}^{1\mathrm{T}} \\ 0 & \cdots & 0 & \cdots \\ 0 & 0 & \alpha_z^s\tilde{\mathbf{M}}^s & -\alpha_z^s\mathbf{C}^{s\mathrm{T}} \\ 0 & \cdots & 0 & \mathbf{H} \end{pmatrix} \begin{pmatrix} \ddot{\mathbf{U}}_{\mathrm{link}}^1 \\ \vdots \\ \ddot{\mathbf{U}}_{\mathrm{link}}^s \\ \Lambda \end{pmatrix} = \begin{pmatrix} 0 \\ \vdots \\ 0 \\ -\sum_{k=1}^s \mathbf{C}^k\mathbf{W}_{z_{\mathrm{free}}}^k \end{pmatrix}, \tag{2.12}$$

where $\mathbf{H}$ is the condensation operator:

$$\mathbf{H} = \sum_{k=1}^{s} \alpha_z^k\mathbf{C}^k\tilde{\mathbf{M}}^{k^{-1}}\mathbf{C}^{k^{\mathrm{T}}}. \tag{2.13}$$

This method can be summarized in the following flow chart for one time-step:

(a) Solve the free problem on each subdomain:

$$\tilde{\mathbf{M}}^k\ddot{\mathbf{U}}_{\mathrm{free}}^k = \mathbf{F}_{\mathrm{ext}}^k - \mathbf{K}^k\,{}^{\mathrm{p}}\mathbf{U}^k \quad \forall k \in \{1,\ldots,s\} \tag{2.14}$$

and

$$\begin{aligned}\dot{\mathbf{U}}^k_{\text{free}} &= {}^{\text{p}}\dot{\mathbf{U}}^k + \alpha_2^k \ddot{\mathbf{U}}^k_{\text{free}},\\ \mathbf{U}^k_{\text{free}} &= {}^{\text{p}}\mathbf{U}^k + \alpha_3^k \ddot{\mathbf{U}}^k_{\text{free}}\end{aligned} \quad \forall k \in \{1,\dots,s\}. \tag{2.15}$$

(b) Calculate the Lagrange multipliers using the condensed global problem:

$$\mathbf{H}\Lambda = -\mathbf{C}\mathbf{W}_{z_{\text{free}}}. \tag{2.16}$$

(c) Solve the link problem on each subdomain:

$$\tilde{\mathbf{M}}^k \ddot{\mathbf{U}}^k_{\text{link}} = \mathbf{C}^{k^{\text{T}}} \Lambda \quad \forall k \in \{1,\dots,s\}. \tag{2.17}$$

(d) Calculate the kinematic quantities of the global problem:

$$\begin{aligned}\ddot{\mathbf{U}}^k &= \ddot{\mathbf{U}}^k_{\text{free}} + \alpha_1^k \ddot{\mathbf{U}}^k_{\text{link}}\\ \dot{\mathbf{U}}^k &= \dot{\mathbf{U}}^k_{\text{free}} + \alpha_2^k \ddot{\mathbf{U}}^k_{\text{link}}\\ \mathbf{U}^k &= \mathbf{U}^k_{\text{free}} + \alpha_3^k \ddot{\mathbf{U}}^k_{\text{link}}\end{aligned} \quad \forall k \in \{1,\dots,s\}. \tag{2.18}$$

Remark.

- If we consider an explicit numerical scheme in subdomain k [11,19,20], the corresponding subdomain quantities must verify $\beta^k = 0$, $\tilde{\mathbf{M}}^k = \mathbf{M}^k$ with $\mathbf{M}^k$ lumped mass matrix.
- The flow chart above, in fact, describes a whole family of algorithms involving continuous displacements, or velocities, or accelerations at the interfaces. For the purpose of comparing these different choices and in order to obtain a necessary condition of convergence, we will study the stability of the scheme in each case using the energy method [11] in Section 3.

2.2. Coupling between Newmark schemes with different time-steps

We will now address the resolution of the discretized problem (1.6) using Eqs. (1.12) and (1.13) in the case of different time-steps in each subdomain. First, we consider two subdomains A and B with linear elastic material behavior. For example, A is an implicit subdomain and B uses an explicit Newmark scheme. By analogy with multi-scale methods in space, we must define a prolongation operator in order to go from the "coarse" timescale (subdomain A, time-step ΔT) to the "fine" timescale (subdomain B, time-step Δt) and a restriction operator to go from the "fine" scale to the "coarse" scale. We will make the assumption that $\Delta T = m\Delta t$. Let us now define the interpolated quantities at time-step j by the linear interpolation:

$$\hat{\mathbf{W}}_{z_j} = \mathbf{W}_{z_0}\left(1 - \frac{j}{m}\right) + \frac{j}{m}\mathbf{W}_{z_m} \quad \text{with } j \in \{1,\dots,m\}, \tag{2.19a}$$

$$\hat{\Lambda}_j = \Lambda_0\left(1 - \frac{j}{m}\right) + \frac{j}{m}\Lambda_m \quad \text{with } j \in \{1,\dots,m\}. \tag{2.19b}$$

We chose to prescribe exact equilibrium through the interface at time-step $\Delta T = [t_0, t_m]$ and continuity of kinematic quantities at time-step $j\Delta t$ (see Fig. 1). Consequently, we have only an approximate equilibrium at time-step $j\Delta t$ because the interface quantities are interpolated.

For time-step $\Delta T = m\Delta t$ we must have

$$\mathbf{M}^A \ddot{\mathbf{U}}^A_m + \mathbf{K}^A \mathbf{U}^A_m = \mathbf{F}^A_{\text{ext}_m} + \mathbf{C}^{A^{\text{T}}} \Lambda_m. \tag{2.20}$$

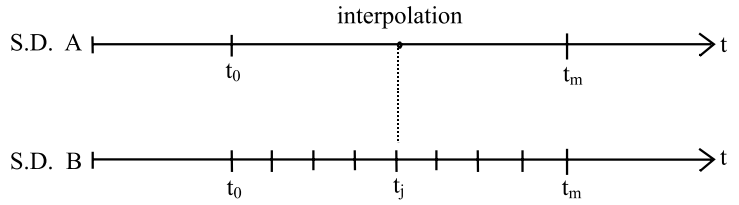

Fig. 1. Definition of the prolongation operator from the coarse timescale to the fine timescale.

For time-step $j\Delta t$ we must have

$$\mathbf{M}^B\ddot{\mathbf{U}}^B_j + \mathbf{K}^B\mathbf{U}^B_j = \mathbf{F}^B_{\mathrm{ext}_j} + \mathbf{C}^{B^{\mathrm{T}}}\hat{\Lambda}_j, \tag{2.21a}$$

$$\mathbf{C}^A\hat{\mathbf{W}}^A_{z_j} + \mathbf{C}^B\mathbf{W}^B_{z_j} = 0. \tag{2.21b}$$

Now, introducing the Newmark scheme for each subdomain A and B, we obtain for the small time-steps $j\Delta t$:

$$\begin{pmatrix} \alpha^B_z\tilde{\mathbf{M}}^B & -\alpha^B_z\mathbf{C}^{B^{\mathrm{T}}} \\ -\alpha^B_z\mathbf{C}^B & 0 \end{pmatrix}\begin{pmatrix} \ddot{\mathbf{U}}^B_j \\ \hat{\Lambda}_j \end{pmatrix} = \begin{pmatrix} \alpha^B_z\left(\mathbf{F}^B_{\mathrm{ext}_j} - \mathbf{K}^{B\,\mathrm{p}}\mathbf{U}^B_{j-1}\right) \\ \mathbf{C}^A\hat{\mathbf{W}}^A_{z_j} + \mathbf{C}^{B\,\mathrm{p}}\mathbf{W}^B_{z_j-1} \end{pmatrix}. \tag{2.22}$$

For the large time-step ΔT we get

$$\begin{pmatrix} \alpha^A_z\tilde{\mathbf{M}}^A & -\alpha^A_z\mathbf{C}^{A^{\mathrm{T}}} \\ -\alpha^A_z\mathbf{C}^A & 0 \end{pmatrix}\begin{pmatrix} \ddot{\mathbf{U}}^A_m \\ \Lambda_m \end{pmatrix} = \begin{pmatrix} \alpha^A_z\left(\mathbf{F}^A_{\mathrm{ext}_m} - \mathbf{K}^{A\,\mathrm{p}}\mathbf{U}^A_0\right) \\ \mathbf{C}^{A\,\mathrm{p}}\mathbf{W}^A_{z_m} + \mathbf{C}^B\mathbf{W}^B_{z_m} \end{pmatrix}. \tag{2.23}$$

As before, we decompose the matrix equations (2.22) and (2.23) into a free problem and a constrained problem. For this purpose, we apply the free/link approach to all the equations of the problem: equilibrium equations, continuity equations at the interface, Newmark equations and scale change operators:

$$\hat{\mathbf{W}}^A_{z_{j_{\mathrm{free}}}} = \left(1 - \frac{j}{m}\right)\mathbf{W}^A_{z_{0_{\mathrm{free}}}} + \frac{j}{m}\mathbf{W}^A_{z_{m_{\mathrm{free}}}}, \tag{2.24a}$$

$$\hat{\mathbf{W}}^A_{z_{j_{\mathrm{link}}}} = \left(1 - \frac{j}{m}\right)\mathbf{W}^A_{z_{0_{\mathrm{link}}}} + \frac{j}{m}\mathbf{W}^A_{z_{m_{\mathrm{link}}}}. \tag{2.24b}$$

Let us now rewrite Eq. (2.21b) using free and link terms:

$$\mathbf{C}^A\hat{\mathbf{W}}^A_{z_{j_{\mathrm{link}}}} + \mathbf{C}^B\mathbf{W}^B_{z_{j_{\mathrm{link}}}} = -\left(\mathbf{C}^A\hat{\mathbf{W}}^A_{z_{j_{\mathrm{free}}}} + \mathbf{C}^B\mathbf{W}^B_{z_{j_{\mathrm{free}}}}\right). \tag{2.25}$$

From (2.24b) and (2.17), we get

$$\hat{\mathbf{W}}^A_{z_{j_{\mathrm{link}}}} = \left(1 - \frac{j}{m}\right)\mathbf{W}^A_{z_{0_{\mathrm{link}}}} + \frac{j}{m}\alpha^A_z\mathbf{M}^{A^{-1}}\mathbf{C}^{A^{\mathrm{T}}}\Lambda_m.$$

Using (2.19b), we obtain

$$\hat{\mathbf{W}}^A_{z_{j_{\mathrm{link}}}} = \left(1 - \frac{j}{m}\right)\left(\mathbf{W}^A_{z_{0_{\mathrm{link}}}} - \alpha^A_z\mathbf{M}^{A^{-1}}\mathbf{C}^{A^{\mathrm{T}}}\Lambda_0\right) + \alpha^A_z\mathbf{M}^{A^{-1}}\mathbf{C}^{A^{\mathrm{T}}}\hat{\Lambda}_j,$$

which, because of the equilibrium at the beginning of the first time-step, gives

$$\hat{\mathbf{W}}^A_{z_{j_{\text{link}}}} = \alpha_z^A \mathbf{M}^{A^{-1}} \mathbf{C}^{A^{\mathrm{T}}} \hat{\Lambda}_j. \tag{2.26}$$

We obtain the free and link problems related to the small time-steps $j\Delta t$:

$$\tilde{\mathbf{M}}^B \ddot{\mathbf{U}}^B_{j_{\text{free}}} = \mathbf{F}^B_{\text{ext}_j} - \mathbf{K}^B {}^{\text{p}}\mathbf{U}^B_{j-1}, \tag{2.27}$$

$$\begin{pmatrix} \alpha_z^B \tilde{\mathbf{M}}^B & -\alpha_z^B \mathbf{C}^{B^{\mathrm{T}}} \\ -\alpha_z^B \mathbf{C}^B & -\alpha_z^A \mathbf{C}^A \mathbf{M}^{A^{-1}} \mathbf{C}^{A^{\mathrm{T}}} \end{pmatrix} \begin{pmatrix} \ddot{\mathbf{U}}^B_{j_{\text{link}}} \\ \hat{\Lambda}_j \end{pmatrix} = \begin{pmatrix} 0 \\ \mathbf{C}^A \hat{\mathbf{W}}^A_{z_{j_{\text{free}}}} + \mathbf{C}^B \mathbf{W}^B_{z_{j_{\text{free}}}} \end{pmatrix} \tag{2.28}$$

and the free and link problems related to the large time-steps ΔT:

$$\tilde{\mathbf{M}}^A \ddot{\mathbf{U}}^A_{m_{\text{free}}} = \mathbf{F}^A_{\text{ext}_m} - \mathbf{K}^A {}^{\text{p}}\mathbf{U}^A_0, \tag{2.29}$$

$$\begin{pmatrix} \alpha_z^A \tilde{\mathbf{M}}^A & -\alpha_z^A \mathbf{C}^{A^{\mathrm{T}}} \\ -\alpha_z^A \mathbf{C}^A & -\alpha_z^B \mathbf{C}^B \mathbf{M}^{B^{-1}} \mathbf{C}^{B^{\mathrm{T}}} \end{pmatrix} \begin{pmatrix} \ddot{\mathbf{U}}^A_{m_{\text{link}}} \\ \Lambda_m \end{pmatrix} = \begin{pmatrix} 0 \\ \mathbf{C}^A \hat{\mathbf{W}}^A_{z_{m_{\text{free}}}} + \mathbf{C}^B \mathbf{W}^B_{z_{m_{\text{free}}}} \end{pmatrix}. \tag{2.30}$$

Remark. The matrix equations (2.28) and (2.30) can be condensed on the interfaces; thus, we obtain for each case a condensation operator of the form:

$$\mathbf{H} = \alpha_z^A \mathbf{C}^A \tilde{\mathbf{M}}^{A^{-1}} \mathbf{C}^{A^{\mathrm{T}}} + \alpha_z^B \mathbf{C}^B \tilde{\mathbf{M}}^{B^{-1}} \mathbf{C}^{B^{\mathrm{T}}}. \tag{2.31}$$

We can also summarize the method in the form of a flow chart for one time-step ΔT:

(a) Solve the free problem for subdomain A at time t_m:

$$\tilde{\mathbf{M}}^A \ddot{\mathbf{U}}^A_{\text{free}} = \mathbf{F}^A_{\text{ext}} - \mathbf{K}^A {}^{\text{p}}\mathbf{U}^A \tag{2.32}$$

and

$$\begin{aligned} \dot{\mathbf{U}}^A_{\text{free}} &= {}^{\text{p}}\dot{\mathbf{U}}^A + \alpha_2^A \ddot{\mathbf{U}}^A_{\text{free}}, \\ \mathbf{U}^A_{\text{free}} &= {}^{\text{p}}\mathbf{U}^A + \alpha_3^A \ddot{\mathbf{U}}^A_{\text{free}}. \end{aligned} \tag{2.33}$$

(b) Loop on the m time-steps of subdomain B at times t_j with $j \in \{1, \ldots, m\}$.

(c) Solve the free problem for subdomain B at time t_j:

$$\tilde{\mathbf{M}}^B \ddot{\mathbf{U}}^B_{\text{free}} = \mathbf{F}^B_{\text{ext}} - \mathbf{K}^B {}^{\text{p}}\mathbf{U}^B \tag{2.34}$$

and

$$\begin{aligned} \dot{\mathbf{U}}^B_{\text{free}} &= {}^{\text{p}}\dot{\mathbf{U}}^B + \alpha_2^B \ddot{\mathbf{U}}^B_{\text{free}}; \\ \mathbf{U}^B_{\text{free}} &= {}^{\text{p}}\mathbf{U}^B + \alpha_3^B \ddot{\mathbf{U}}^B_{\text{free}}. \end{aligned} \tag{2.35}$$

(d) Change scale for the kinematic quantities of subdomain A:

$$\hat{\mathbf{W}}^A_{z_{j_{\text{free}}}} = \left(1 - \frac{j}{m}\right) \mathbf{W}^A_{z_{0_{\text{free}}}} + \frac{j}{m} \mathbf{W}^A_{z_{m_{\text{free}}}}. \tag{2.36}$$

(e) Calculate the Lagrange multipliers using the condensed global problem:

$$\mathbf{H}\Lambda = -\left(\mathbf{C}^A \hat{\mathbf{W}}^A_{z_{\text{free}}} + \mathbf{C}^B \mathbf{W}^B_{z_{\text{free}}}\right). \tag{2.37}$$

(f) Solve the link problem of subdomain B:

$$\mathbf{M}^B\ddot{\mathbf{U}}^B_{\text{link}} = \mathbf{C}^{B^{\mathrm{T}}}\Lambda. \tag{2.38}$$

(g) Calculate the kinematic quantities of subdomain B:

$$\begin{aligned}
\ddot{\mathbf{U}}^B &= \ddot{\mathbf{U}}^B_{\text{free}} + \alpha_1^B\ddot{\mathbf{U}}^B_{\text{link}};\\
\dot{\mathbf{U}}^B &= \dot{\mathbf{U}}^B_{\text{free}} + \alpha_2^B\ddot{\mathbf{U}}^B_{\text{link}};\\
\mathbf{U}^B &= \mathbf{U}^B_{\text{free}} + \alpha_3^B\ddot{\mathbf{U}}^B_{\text{link}}.
\end{aligned} \tag{2.39}$$

(h) If $j = m$, then end of loop.
(i) Solve the link problem of subdomain A:

$$\mathbf{M}^A\ddot{\mathbf{U}}^A_{\text{link}} = \mathbf{C}^{A^{\mathrm{T}}}\Lambda. \tag{2.40}$$

(j) Calculate the kinematic quantities of subdomain A:

$$\begin{aligned}
\ddot{\mathbf{U}}^A &= \ddot{\mathbf{U}}^A_{\text{free}} + \alpha_1^A\ddot{\mathbf{U}}^A_{\text{link}};\\
\dot{\mathbf{U}}^A &= \dot{\mathbf{U}}^A_{\text{free}} + \alpha_2^A\ddot{\mathbf{U}}^A_{\text{link}};\\
\mathbf{U}^A &= \mathbf{U}^A_{\text{free}} + \alpha_3^A\ddot{\mathbf{U}}^A_{\text{link}}.
\end{aligned} \tag{2.41}$$

The method can be generalized to s subdomains with the following assumption:

$$\begin{aligned}
&\Delta t_1 = \Delta t,\\
&\Delta t_2 = m_2\Delta t,\\
&\quad\vdots\\
&\Delta t_s = m_s\Delta t
\end{aligned} \tag{2.42}$$

with $\{m_2,\ldots,m_s\} \in N^{*s-1}$.
The algorithm is rather complex but can be implemented.

Remarks and conclusions.

- The condensation operator at the interfaces is constant and independent of j. Therefore, in the geometrically linear case, it needs to be calculated only once at the beginning of the dynamic calculation.
- As in Section 1.2, this algorithm leads to a whole family of algorithms. Actually, many of these schemes can be numerically unstable. We will prove in Section 3.3 that if we choose velocity continuity at the interfaces and interpolation of velocities with time, the corresponding numerical scheme is stable for any Newmark scheme.

3. Stability and convergence analysis

Usually, the stability of a numerical scheme is studied from the evolution of the state vector through the characteristic matrix of the numerical scheme. Two types of state vectors are generally considered:

$$\mathbf{Y}_n = \begin{bmatrix}\mathbf{U}_n\\ \dot{\mathbf{U}}_n\end{bmatrix} \quad\text{and}\quad \mathbf{Y}_n = \begin{bmatrix}\mathbf{U}_n\\ \dot{\mathbf{U}}_n\\ \ddot{\mathbf{U}}_n\end{bmatrix}. \tag{3.1}$$

Farhat [21] shows that if we use a hybrid formulation, such as Schur's dual formulations, to connect the subdomains and if the link energy is zero, the stability and the accuracy of the Newmark scheme in each subdomain are not affected by the interfaces. Hence, if we now use Hughes' results [11], the damping ratio in each subdomain is

$$\xi_k = \pi\left(\gamma_k - \tfrac{1}{2}\right)\frac{\Delta t_k}{T} + \mathrm{o}\left(\left(\frac{\Delta t_k}{T}\right)^2\right). \tag{3.2}$$

If we consider only subdomains such that $\gamma_k = 1/2$ and if the interface energy is zero, the accuracy of the coupled problem is of the second order. If one of the subdomains is such that $\gamma_k \neq 1/2$, the accuracy of the whole coupled problem is of the first order at most. We will now study the stability of the coupled schemes in greater depth. In the following sections, we will study the stability of the different cases considered above using an energy method to extend the results of [11].

3.1. Presentation of the method

In this paper, we will use an energy method developed by Hughes [11]. For this purpose, we will use the following notations:

$$\langle \mathbf{A}_n \rangle = (\mathbf{A}_n + \mathbf{A}_{n+1})/2, \tag{3.3}$$

$$[\mathbf{A}_n] = (\mathbf{A}_{n+1} - \mathbf{A}_n) \tag{3.4}$$

with the property:

$$\langle \mathbf{A}_n \rangle \cdot [\mathbf{A}_n] = \left[\tfrac{1}{2}\mathbf{A}_n^2\right]. \tag{3.5}$$

In order to derive the energy formulation, we consider the following expression obtained from (1.2) and (2.5):

$$\left[\dot{\mathbf{U}}_n\right]^{\mathrm{T}}\left(\mathbf{M}\left[\ddot{\mathbf{U}}_n\right] + \mathbf{K}[\mathbf{U}_n] - [\mathbf{F}_{\mathrm{ext}_n}]\right) = 0 \tag{3.6}$$

or, in a form adapted to the Newmark numerical scheme:

$$[\mathbf{U}_n] = \Delta t\left\langle \dot{\mathbf{U}}_n \right\rangle + \tfrac{1}{2}\Delta t^2(2\beta - \gamma)\left[\ddot{\mathbf{U}}_n\right], \tag{3.7a}$$

$$\left[\dot{\mathbf{U}}_n\right] = \Delta t\left\langle \ddot{\mathbf{U}}_n \right\rangle + \Delta t\left(\gamma - \tfrac{1}{2}\right)\left[\ddot{\mathbf{U}}_n\right]. \tag{3.7b}$$

From Eqs. (3.5), (3.6) and (3.7a) and (3.7b), we get

$$\left(\tfrac{1}{2}\ddot{\mathbf{U}}_{n+1}^{\mathrm{T}}\mathbf{A}\ddot{\mathbf{U}}_{n+1} - \tfrac{1}{2}\ddot{\mathbf{U}}_n^{\mathrm{T}}\mathbf{A}\ddot{\mathbf{U}}_n\right) + \left(\tfrac{1}{2}\dot{\mathbf{U}}_{n+1}^{\mathrm{T}}\mathbf{K}\dot{\mathbf{U}}_{n+1} - \tfrac{1}{2}\dot{\mathbf{U}}_n^{\mathrm{T}}\mathbf{K}\dot{\mathbf{U}}_n\right) = -\left(\gamma - \tfrac{1}{2}\right)\left[\ddot{\mathbf{U}}_n\right]^{\mathrm{T}}\mathbf{A}\left[\ddot{\mathbf{U}}_n\right] + \frac{1}{\Delta t}\left[\dot{\mathbf{U}}_n\right]^{\mathrm{T}}[\mathbf{F}_n] \tag{3.8}$$

with

- $[T(\ddot{\mathbf{U}}_n)] = (\tfrac{1}{2}\ddot{\mathbf{U}}_{n+1}^{\mathrm{T}}\mathbf{A}\ddot{\mathbf{U}}_{n+1} - \tfrac{1}{2}\ddot{\mathbf{U}}_n^{\mathrm{T}}\mathbf{A}\ddot{\mathbf{U}}_n)$ term related to the variation of kinetic energy;
- $[V(\dot{\mathbf{U}}_n)] = (\tfrac{1}{2}\dot{\mathbf{U}}_{n+1}^{\mathrm{T}}\mathbf{K}\dot{\mathbf{U}}_{n+1} - \tfrac{1}{2}\dot{\mathbf{U}}_n^{\mathrm{T}}\mathbf{K}\dot{\mathbf{U}}_n)$ term related to the variation of strain energy;
- $-D([\ddot{\mathbf{U}}_n]) = -(\gamma - \tfrac{1}{2})[\ddot{\mathbf{U}}_n]^{\mathrm{T}}\mathbf{A}[\ddot{\mathbf{U}}_n]$ term related to numerical damping;
- $E_{\mathrm{ext}}([\dot{\mathbf{U}}_n]) = 1/\Delta t[\dot{\mathbf{U}}_n]^{\mathrm{T}}[\mathbf{F}_{\mathrm{ext}_n}]$ term related to the work due to the external forces.
- $\mathbf{A} = \mathbf{M} + \tfrac{1}{2}\Delta t^2(2\beta - \gamma)\mathbf{K}$ (3.9)

Remark. In the following discussion, we will disregard the term related to the work due to the external forces, since this term has no impact on the stability of the scheme [7].

Theorem 1. *If* $\gamma \geqslant 1/2$ *and* $\mathbf{A}$ *is positive definite, then* $\ddot{\mathbf{U}}_{n+1}$ *and* $\dot{\mathbf{U}}_{n+1}$ *are bounded* (*see* [11] *for proof*).

Consequence. If Theorem 1 is verified and $\mathbf{K}^{-1}$ exists, then $\mathbf{U}_{n+1}$ is also bounded (from (1.2) and (2.5)).

The advantage of this formulation and this theorem is that one can study the stability of the Newmark numerical scheme directly from $\mathbf{A}$ because if one uses the eigenmodes to diagonalize $\mathbf{A}$ one gets the following second-degree inequation in Δt:

$$1 + \left(\beta - \tfrac{1}{2}\gamma\right)\left(\omega^h \Delta t\right)^2 \geqslant 0, \tag{3.10}$$

where ω^h are the eigenvalues of $\mathbf{A}$ matrix. Then, the method gives the following results:

$$\tfrac{1}{2} \leqslant \gamma \leqslant 2\beta \text{ unconditionally stable method} \tag{3.11}$$

$$\tfrac{1}{2} \leqslant \gamma \quad \text{and} \quad 2\beta \leqslant \gamma \text{ conditionally stable method} \quad \Delta t \leqslant \frac{1}{\omega\sqrt{(\gamma/2) - \beta}} \tag{3.12}$$

where, by definition, $\omega = \sup\{\omega^h\}$. The numerical damping term also allows us to conclude that if $\gamma = 1/2$ the numerical scheme has no damping; on the contrary, $\gamma > 1/2$, the scheme dissipates energy.

Remark. It is possible to take mechanical damping into account. In this case, Eq. (3.8) contains a new term related to mechanical damping. Besides, the term related to numerical damping is different. In this respect, we go back to the classical stability properties of Newmark schemes with mechanical damping [11].

3.2. Stability analysis of the algorithm with s subdomains and one time-step Δt

Now, we assume that the structure is divided into subdomains. We want to find a way to discretize the links without affecting the precision and stability of the numerical schemes in each subdomain:

- If we produce energy at the interface we get numerical instability.
- If we dissipate energy, we get artificial damping resulting in stability, but we lose precision.

The "energy" of the whole system of s subdomains and their interfaces is

$$\sum_{k=1}^{s}\left[T^k\left(\ddot{\mathbf{U}}_n^k\right)\right] + \sum_{k=1}^{s}\left[V^k\left(\dot{\mathbf{U}}_n^k\right)\right] = -\sum_{k=1}^{s} D^k([\ddot{\mathbf{U}}_n^k]) + \sum_{k=1}^{s}\frac{1}{\Delta t}\left[\dot{\mathbf{U}}_n^k\right]^{\mathrm{T}}\mathbf{C}^{k^{\mathrm{T}}}[\Lambda_n], \tag{3.13}$$

where the interface term is represented by the Lagrange multipliers:

$$E_{\mathrm{link}}([\mathbf{W}_n^k]) = \sum_{k=1}^{s}\frac{1}{\Delta t}\left[\dot{\mathbf{U}}_n^k\right]^{\mathrm{T}}\mathbf{C}^{k^{\mathrm{T}}}[\Lambda_n] = \frac{1}{\Delta t}[\Lambda_n]^{\mathrm{T}}\left(\sum_{k=1}^{s}\mathbf{C}^k\left[\dot{\mathbf{U}}_n^k\right]\right). \tag{3.14}$$

We are restricting ourselves to cases where the interface energy is zero. This choice preserves the precision of the Newmark schemes in each subdomain. We must point out that roundoff errors resulting from the numerical solution of the interface problem can affect the stability and the convergence of the whole system. Should this problem arise, the introduction of a controlled dissipative time integration scheme such as HHT or the α-method could be used [22,23]. The advantage of this presentation is that it enables us to conclude rapidly on the stability of the numerical scheme depending on the various kinematic assumptions at the interface.

Case 1: Continuity of accelerations

$$\sum_{k=1}^{s} \mathbf{C}^k \ddot{\mathbf{U}}^k = 0. \tag{3.15}$$

Using (3.7b), one can write

$$\sum_{k=1}^{s} \mathbf{C}^k \left[\dot{\mathbf{U}}_n^k\right] = \Delta t \sum_{k=1}^{s} \mathbf{C}^k \left\langle \ddot{\mathbf{U}}_n^k \right\rangle + \Delta t \sum_{k=1}^{s} \left(\gamma_k - \tfrac{1}{2}\right) \mathbf{C}^k \left[\ddot{\mathbf{U}}_n^k\right]. \tag{3.16}$$

Furthermore, if $\gamma_k = \gamma_0 \ \forall k \in \{1, \ldots, s\}$, we get

$$\sum_{k=1}^{s} \mathbf{C}^k \left[\dot{\mathbf{U}}_n^k\right] = \Delta t \sum_{k=1}^{s} \mathbf{C}^k \left\langle \ddot{\mathbf{U}}_n^k \right\rangle + \left(\gamma_0 - \tfrac{1}{2}\right) \Delta t \sum_{k=1}^{s} \mathbf{C}^k \left[\ddot{\mathbf{U}}_n^k\right]. \tag{3.17}$$

The assumption of continuous accelerations at the interface (3.15) yields:

$$\begin{aligned} &\sum_{k=1}^{s} \mathbf{C}^k \left\langle \ddot{\mathbf{U}}_n^k \right\rangle = 0, \\ &\sum_{k=1}^{s} \mathbf{C}^k \left[\ddot{\mathbf{U}}_n^k\right] = 0. \end{aligned} \tag{3.18}$$

Then, from (3.17) and (3.18)

$$\sum_{k=1}^{s} \mathbf{C}^k \left[\dot{\mathbf{U}}_n^k\right] = 0. \tag{3.19}$$

Hence, if $\gamma_k = \gamma_0 \ \forall k \in \{1, \ldots, s\}$, each subdomain's stability condition is unchanged and

$$E_{\text{link}} = 0. \tag{3.20}$$

Conclusion: We can observe that if all numerical schemes have the same γ_k, the stability of the numerical scheme is affected only by roundoff errors associated with the computation of the condition of acceleration continuity at the interfaces. Similarly, the stability and the accuracy of the method are related only to the time discretization of each subdomain. For instance, we can couple the following second-order numerical schemes:

$$\begin{aligned} &\gamma_1 = \tfrac{1}{2}, \quad \beta_1 = \tfrac{1}{4} \qquad \text{(implicit, unconditionally stable)}, \\ &\gamma_2 = \tfrac{1}{2}, \quad \beta_2 = 0 \qquad \text{(explicit, conditionally stable)} \end{aligned} \tag{3.21}$$

using the expression of the damping ratio defined by [11]:

$$\xi_k = \pi\left(\gamma_k - \tfrac{1}{2}\right) \frac{\Delta t_k}{T} + \mathrm{o}\left(\left(\frac{\Delta t_k}{T}\right)^2\right). \tag{3.22}$$

In this case, we should then preserve second order accuracy.

Case 2: Continuity of velocities

$$\sum_{k=1}^{s} \mathbf{C}^k \dot{\mathbf{U}}^k = 0. \tag{3.23}$$

The assumption of continuous velocities at the interface yields

$$\sum_{k=1}^{s} \mathbf{C}^k \left[\dot{\mathbf{U}}_n^k \right] = 0. \tag{3.24}$$

Conclusion: As in the previous case, the stability of the numerical scheme, regardless of the set of parameters of the Newmark scheme in each subdomain, is affected only by roundoff errors coming from the condition of continuity of velocities at the interfaces.

Case 3: Continuity of displacements

$$\sum_{k=1}^{s} \mathbf{C}^k \mathbf{U}^k = 0. \tag{3.25}$$

From expression (3.7a), we can write

$$\sum_{k=1}^{s} \mathbf{C}^k \left[\mathbf{U}_n^k \right] = \Delta t \sum_{k=1}^{s} \mathbf{C}^k \left\langle \dot{\mathbf{U}}_n^k \right\rangle + \tfrac{1}{2}\Delta t^2 \sum_{k=1}^{s} (2\beta_k - \gamma_k) \mathbf{C}^k \left[\ddot{\mathbf{U}}_n^k \right]. \tag{3.26}$$

This expression shows that the parameters of the numerical scheme influence stability. Thus, we will study the conditions which must be satisfied in order for the displacements to be acceptably continuous. If we assume that for each subdomain $\gamma_k = 2\beta_k$ (for example: $\gamma = 1/2,\ \beta = 1/4$), we get

$$\sum_{k=1}^{s} \mathbf{C}^k \left[\mathbf{U}_n^k \right] = \Delta t \sum_{k=1}^{s} \mathbf{C}^k \left\langle \dot{\mathbf{U}}_n^k \right\rangle = 0, \tag{3.27}$$

therefore

$$\sum_{k=1}^{s} \mathbf{C}^k \dot{\mathbf{U}}_{n+1}^k = -\sum_{k=1}^{s} \mathbf{C}^k \dot{\mathbf{U}}_n^k. \tag{3.28}$$

If we now assume continuity of velocities at $t = 0$, from expression (3.28), we get

$$\sum_{k=1}^{s} \mathbf{C}^k \dot{\mathbf{U}}_0^k = 0 \ \Rightarrow\ \sum_{k=1}^{s} \mathbf{C}^k \dot{\mathbf{U}}_n^k = 0 \ \Rightarrow\ \sum_{k=1}^{s} \mathbf{C}^k \dot{\mathbf{U}}_{n+1}^k = 0, \tag{3.29}$$

therefore

$$\sum_{k=1}^{s} \mathbf{C}^k \left[\dot{\mathbf{U}}_n^k \right] = 0. \tag{3.30}$$

In conclusion: if $\gamma_k = 2\beta_k$ and $\sum_{k=1}^{s} \mathbf{C}^k \dot{\mathbf{U}}_0^k = 0$, the stability condition of all subdomains is not altered.

For example: $\gamma_k = 1/2,\ \beta_k = 1/4\ \forall k \in \{1, \ldots, s\}$.

Remark.

- The use of Schur's dual formulation to model interfaces does not modify the accuracy of the Newmark schemes considered in each subdomain [21].
- A specific study [21] showed that if we consider continuous displacements at the interfaces, we can observe a slight instability of the accelerations (with no noticeable consequence on displacements or velocities). In this case, numerical damping can be introduced, for example with the HHT scheme, in order to preserve second-order accuracy.
- If we prescribe continuity of displacements at interfaces with identical time-steps, we cannot couple standard explicit or implicit numerical schemes with zero energy at the interface. On the other hand,

continuity of accelerations and velocities at the interfaces yields two possible stable schemes for coupling explicit and implicit subdomains with equal time-steps.

3.3. Stability study of the algorithm with different time-steps

The objective of this work is to show that continuity of velocities at the interfaces along with linear interpolation of the velocities results in a stable algorithm which allows us to couple numerical schemes of the Newmark family with different time-steps. We will also use the following generalized notations:

$$\langle\langle \mathbf{A}_0 \rangle\rangle = (\mathbf{A}_0 + \mathbf{A}_m)/2, \tag{3.31}$$

$$[[\mathbf{A}_0]] = (\mathbf{A}_m - \mathbf{A}_0). \tag{3.32}$$

Let us write Eq. (3.13) for subdomain A:

$$[[T^A(\ddot{\mathbf{U}}_0^A)]] + [[V^A(\dot{\mathbf{U}}_0^A)]] = -D^A([[\ddot{\mathbf{U}}^A]]) + \frac{1}{m\Delta t}[[\dot{\mathbf{U}}_0^A]]^{\mathrm{T}}\mathbf{C}^{A^{\mathrm{T}}}[[\Lambda_0]]. \tag{3.33}$$

Similarly, let us write (3.13) for subdomain B with time duration $[t_0, t_m]$:

$$[[T^B(\ddot{\mathbf{U}}_0^B)]] + [[V^B(\dot{\mathbf{U}}_0^B)]] = -\sum_{j=1}^{m} D^B([\ddot{\mathbf{U}}_{j-1}^B]) + \sum_{j=1}^{m} \frac{1}{\Delta t}\left[\dot{\mathbf{U}}_{j-1}^B\right]^{\mathrm{T}}\mathbf{C}^{B^{\mathrm{T}}}\left[\hat{\Lambda}_{j-1}\right] \tag{3.34}$$

with the notation

$$\sum_{j=1}^{m}\left[\mathbf{A}_{j-1}\right] = [[\mathbf{A}_0]]. \tag{3.35}$$

Finally, in order to study the stability of the algorithm, we can apply the energy method to the whole structure, i.e. both subdomains A and B and their interface

$$([[T^A]] + [[T^B]]) + ([[V^A]] + [[V^B]]) = -D^A - \sum_{j=1}^{m} D^B([\ddot{\mathbf{U}}_{j-1}^B]) + E_{\mathrm{link}} \tag{3.36}$$

with the interface term

$$E_{\mathrm{link}} = E_{\mathrm{link}}^A + E_{\mathrm{link}}^B = \frac{1}{m\Delta t}[[\dot{\mathbf{U}}_0^A]]^{\mathrm{T}}\mathbf{C}^{A^{\mathrm{T}}}[[\Lambda_0]] + \sum_{j=1}^{m}\frac{1}{\Delta t}\left[\dot{\mathbf{U}}_{j-1}^B\right]^{\mathrm{T}}\mathbf{C}^{B^{\mathrm{T}}}\left[\hat{\Lambda}_{j-1}\right]. \tag{3.37}$$

The condition

$$E_{\mathrm{link}} \leqslant 0 \tag{3.38}$$

ensures that the stability of the different schemes is not affected by the interface.

Furthermore, we will need an adapted form, obtained from expression (2.24a), of the linear interpolation condition for unconstrained velocities:

$$\left[\hat{\dot{\mathbf{U}}}_{j-1_{\mathrm{free}}}^A\right] = \frac{1}{m}[[\dot{\mathbf{U}}_{0_{\mathrm{free}}}^A]]. \tag{3.39}$$

First, we separate the free velocities from the constrained velocities:

$$E_{\text{link}} = \frac{1}{m\Delta t}[[\dot{\mathbf{U}}^{A}_{0_{\text{link}}}]]^{\mathrm{T}}\mathbf{C}^{A^{\mathrm{T}}}[[\Lambda_0]] + \sum_{j=1}^{m}\frac{1}{\Delta t}\left[\dot{\mathbf{U}}^{B}_{j-1_{\text{link}}}\right]^{\mathrm{T}}\mathbf{C}^{B^{\mathrm{T}}}\left[\hat{\Lambda}_{j-1}\right] + \frac{1}{m\Delta t}[[\dot{\mathbf{U}}^{A}_{0_{\text{free}}}]]^{\mathrm{T}}\mathbf{C}^{A^{\mathrm{T}}}[[\Lambda_0]] + \sum_{j=1}^{m}\frac{1}{\Delta t}\left[\dot{\mathbf{U}}^{B}_{j-1_{\text{free}}}\right]^{\mathrm{T}}\mathbf{C}^{B^{\mathrm{T}}}\left[\hat{\Lambda}_{j-1}\right]. \tag{3.40}$$

Then, we can modify the unconstrained terms using expression (3.35) applied to Lagrange multipliers and expression (3.39):

$$E_{\text{link}} = \frac{1}{m\Delta t}[[\dot{\mathbf{U}}^{A}_{0_{\text{link}}}]]^{\mathrm{T}}\mathbf{C}^{A^{\mathrm{T}}}[[\Lambda_0]] + \sum_{j=1}^{m}\frac{1}{\Delta t}\left[\dot{\mathbf{U}}^{B}_{j-1_{\text{link}}}\right]^{\mathrm{T}}\mathbf{C}^{B^{\mathrm{T}}}\left[\hat{\Lambda}_{j-1}\right] + \sum_{j=1}^{m}\frac{1}{\Delta t}\left(\mathbf{C}^{A}\left[\hat{\dot{\mathbf{U}}}^{A}_{j-1_{\text{free}}}\right] + \mathbf{C}^{B}\left[\dot{\mathbf{U}}^{B}_{j-1_{\text{free}}}\right]\right)^{\mathrm{T}}\left[\hat{\Lambda}_{j-1}\right]. \tag{3.41}$$

The continuity of velocities (2.25) allows us to express the free terms as functions of the constrained quantities:

$$E_{\text{link}} = \frac{1}{m\Delta t}[[\dot{\mathbf{U}}^{A}_{0_{\text{link}}}]]^{\mathrm{T}}\mathbf{C}^{A^{\mathrm{T}}}[[\Lambda_0]] + \sum_{j=1}^{m}\frac{1}{\Delta t}\left[\dot{\mathbf{U}}^{B}_{j-1_{\text{link}}}\right]^{\mathrm{T}}\mathbf{C}^{B^{\mathrm{T}}}\left[\hat{\Lambda}_{j-1}\right] - \sum_{j=1}^{m}\frac{1}{\Delta t}\left(\mathbf{C}^{A}\left[\hat{\dot{\mathbf{U}}}^{A}_{j-1_{\text{link}}}\right] + \mathbf{C}^{B}\left[\dot{\mathbf{U}}^{B}_{j-1_{\text{link}}}\right]\right)^{\mathrm{T}}\left[\hat{\Lambda}_{j-1}\right]. \tag{3.42}$$

Therefore, we obtain

$$E_{\text{link}} = \frac{1}{m\Delta t}[[\dot{\mathbf{U}}^{A}_{0_{\text{link}}}]]^{\mathrm{T}}\mathbf{C}^{A^{\mathrm{T}}}[[\Lambda_0]] - \sum_{j=1}^{m}\frac{1}{\Delta t}\left[\hat{\dot{\mathbf{U}}}^{A}_{j-1_{\text{link}}}\right]^{\mathrm{T}}\mathbf{C}^{A^{\mathrm{T}}}\left[\hat{\Lambda}_{j-1}\right]. \tag{3.43}$$

Expression (2.26) also yields

$$\mathbf{C}^{A^{\mathrm{T}}}\hat{\Lambda}_j = \frac{1}{\alpha_2^{A}}\tilde{\mathbf{M}}^{A}\dot{\mathbf{U}}^{A}_{j_{\text{link}}}. \tag{3.44}$$

Finally

$$E_{\text{link}} = \frac{1}{\gamma_A}\left(\frac{[[\dot{\mathbf{U}}^{A}_{0_{\text{link}}}]]^{\mathrm{T}}}{m\Delta t}\tilde{\mathbf{M}}^{A}\frac{[[\dot{\mathbf{U}}^{A}_{0_{\text{link}}}]]}{m\Delta t} - \frac{1}{m}\sum_{j=1}^{m}\frac{\left[\hat{\dot{\mathbf{U}}}^{A}_{j-1_{\text{link}}}\right]^{\mathrm{T}}}{\Delta t}\tilde{\mathbf{M}}^{A}\frac{\left[\hat{\dot{\mathbf{U}}}^{A}_{j-1_{\text{link}}}\right]}{\Delta t}\right). \tag{3.45}$$

In order to conclude on the stability of this scheme, we will study the sign of expression (3.45). For this purpose, we will consider the matrix problem in an equivalent scalar form:

$$\tilde{E}^{m}_{\text{link}} = (\alpha_{n+m} - \alpha_n)^2 - m\sum_{j=1}^{m}(\alpha_{n+j} - \alpha_{n+j-1})^2. \tag{3.46}$$

In the case $m = 2$:

$$\tilde{E}^{2}_{\text{link}} = (\alpha_{n+2} - \alpha_n)^2 - 2\sum_{j=1}^{2}(\alpha_{n+j} - \alpha_{n+j-1})^2, \tag{3.47}$$

we get

$$\tilde{E}^{2}_{\text{link}} = -((\alpha_{n+2} - \alpha_{n+1}) - (\alpha_{n+1} - \alpha_n))^2. \tag{3.48}$$

In the case $m = 3$:

$$\tilde{E}^3_{\text{link}} = (\alpha_{n+3} - \alpha_n)^2 - 3\sum_{j=1}^{3} (\alpha_{n+j} - \alpha_{n+j-1})^2, \tag{3.49}$$

we get

$$\begin{aligned}\tilde{E}^3_{\text{link}} = &-((\alpha_{n+3} - \alpha_{n+2}) - (\alpha_{n+2} - \alpha_{n+1}))^2 - ((\alpha_{n+3} - \alpha_{n+2}) - (\alpha_{n+1} - \alpha_n))^2 - ((\alpha_{n+2} - \alpha_{n+1}) \\ &- (\alpha_{n+1} - \alpha_n))^2.\end{aligned} \tag{3.50}$$

Finally, we can show that, at any rank m, we have the following expression, which consists of $(m(m-1))/2$ terms:

$$\begin{aligned}\tilde{E}^m_{\text{link}} = &-((\alpha_{n+m} - \alpha_{n+m-1}) - (\alpha_{n+m-1} - \alpha_{n+m-2}))^2 - ((\alpha_{n+m} - \alpha_{n+m-1}) - (\alpha_{n+m-2} - \alpha_{n+m-3}))^2 \\ &- \cdots - ((\alpha_{n+m} - \alpha_{n+m-1}) - (\alpha_{n+1} - \alpha_n))^2 - ((\alpha_{n+m-1} - \alpha_{n+m-2}) - (\alpha_{n+m-2} - \alpha_{n+m-3}))^2 \\ &- \cdots - ((\alpha_{n+m-1} - \alpha_{n+m-2}) - (\alpha_{n+1} - \alpha_n))^2 - \cdots - ((\alpha_{n+2} - \alpha_{n+1}) - (\alpha_{n+1} - \alpha_n))^2.\end{aligned} \tag{3.51}$$

Therefore, we see that expression (3.45) is a sum of negative squares defined as

$$\begin{aligned}E_{\text{link}} = -\frac{1}{\gamma_A}\sum_{i=1}^{m-1}\sum_{j=i}^{m-1}\Bigg(&\frac{\left(\left(\dot{\mathbf{U}}^A_{m-i+1_{\text{link}}} - \dot{\mathbf{U}}^A_{m-i_{\text{link}}}\right) - \left(\dot{\mathbf{U}}^A_{m-j_{\text{link}}} - \dot{\mathbf{U}}^A_{m-j-1_{\text{link}}}\right)\right)^{\mathrm{T}}}{2\Delta t}\ \tilde{\mathbf{M}}^A \\ &\times \frac{\left(\left(\dot{\mathbf{U}}^A_{m-i+1_{\text{link}}} - \dot{\mathbf{U}}^A_{m-i_{\text{link}}}\right) - \left(\dot{\mathbf{U}}^A_{m-j_{\text{link}}} - \dot{\mathbf{U}}^A_{m-j-1_{\text{link}}}\right)\right)}{2\Delta t}\Bigg).\end{aligned} \tag{3.52}$$

Theorem 2. *If the conditions of Theorem* 1 *are verified for the two subdomains A and B and if* $\tilde{\mathbf{M}}^A$ *is positive definite, then* $\ddot{\mathbf{U}}^A_m, \dot{\mathbf{U}}^A_m, \ddot{\mathbf{U}}^B_m, \dot{\mathbf{U}}^B_m$ *are bounded.*

Elements of Proof. Let us assume that $\gamma_A \geqslant 1/2,\ \gamma_B \geqslant 1/2, \mathbf{A}_A$ is positive definite and $\mathbf{A}_B$ is positive definite (from (3.9)). In this respect, for each subdomain, the stability conditions are defined by (3.11) and (3.12). Therefore, $\tilde{\mathbf{M}}^A$ is positive definite (a necessary and sufficient condition is given by $\beta_A \geqslant 0$, from (2.7).) From Eq. (3.36), with a reasoning similar to that of Theorem 1, we conclude that $\ddot{\mathbf{U}}^A_m, \dot{\mathbf{U}}^A_m, \ddot{\mathbf{U}}^B_m, \dot{\mathbf{U}}^B_m$ are bounded. □

Therefore, if Theorem 2 is verified and $\mathbf{K}^{A^{-1}}$ and $\mathbf{K}^{B^{-1}}$ exist, then $\mathbf{U}^A_m$ and $\mathbf{U}^B_m$ are also bounded (from (2.20) with $\mathbf{F}^A = 0$, $\mathbf{F}^B = 0$, and (2.33)).

Remark.

- The stability of the global problem depends on the stability conditions of the Newmark numerical schemes considered in each subdomain. In this respect, the rate of convergence of the Newmark numerical schemes is defined by (3.22). Therefore, the global accuracy ratio is, at most, equal to the minimum accuracy ratio among all schemes. Then, if the interface energy is zero, we can use parameters (3.21) to couple implicit or explicit numerical schemes with second-order convergence for each.

- Thus, we conclude that the numerical scheme is stable, but can be dissipative (from (3.53)) if the interpolated curve departs too much from a straight line. Regarding this point, if we examine the case $m = 2$, we get from Eq. (3.47):

$$E_{\text{link}} = -\frac{1}{\gamma_A}\left(\frac{\left(\left(\dot{\mathbf{U}}^A_{2_{\text{link}}} - \hat{\dot{\mathbf{U}}}^A_{1_{\text{link}}}\right) - \left(\hat{\dot{\mathbf{U}}}^A_{1_{\text{link}}} - \dot{\mathbf{U}}^A_{0_{\text{link}}}\right)\right)^{\mathrm{T}}}{2\Delta t}\ \tilde{\mathbf{M}}^A \frac{\left(\left(\dot{\mathbf{U}}^A_{2_{\text{link}}} - \hat{\dot{\mathbf{U}}}^A_{1_{\text{link}}}\right) - \left(\hat{\dot{\mathbf{U}}}^A_{1_{\text{link}}} - \dot{\mathbf{U}}^A_{0_{\text{link}}}\right)\right)}{2\Delta t}\right), \tag{3.53}$$

i.e.

$$E_{\text{link}} = -\frac{1}{\gamma_A}\left(\frac{\left(\left[\hat{\dot{\mathbf{U}}}^A_{1_{\text{link}}}\right] - \left[\hat{\dot{\mathbf{U}}}^A_{0_{\text{link}}}\right]\right)^{\mathrm{T}}}{2\Delta t}\ \tilde{\mathbf{M}}^A \frac{\left(\left[\hat{\dot{\mathbf{U}}}^A_{1_{\text{link}}}\right] - \left[\hat{\dot{\mathbf{U}}}^A_{0_{\text{link}}}\right]\right)}{2\Delta t}\right). \tag{3.54}$$

This can be interpreted geometrically as showed in Fig. 2: Fig. 2 and Eq. (3.53) show that for any ratio of time-steps between subdomain A and subdomain B, the numerical scheme dissipates energy in zones where the radius of curvature is small, i.e. where the linear interpolation is not very good.

Finally, with this approach, coupling between different numerical schemes of the Newmark family does not alter the stability of these schemes. Therefore, implicit subdomains remain unconditionally stable and explicit subdomains remain conditionally stable with the same stability limits. Finally, one can conclude from this result that the ratio of the time-step of subdomain A to the time-step of subdomain B has no effect on the stability of the scheme; on the other hand, this parameter is conditioned by the quality of the interpolation of kinematic quantities for subdomain A, on which the numerical damping of the method depends directly.

3.4. Adaptation of the algorithm with different time-steps to problems with material nonlinearities

In this section, A is associated with an implicit scheme and B with an explicit scheme. We consider geometric and material nonlinearities in the explicit subdomain only. We choose the following parameters for subdomains A and B:

$$\gamma_A = \tfrac{1}{2} \quad \text{and} \quad \beta_A = \tfrac{1}{4} \qquad \text{(implicit, second-order numerical scheme)}, \tag{3.55}$$

$$\gamma_B = \tfrac{1}{2} \quad \text{and} \quad \beta_B = 0 \qquad \text{(explicit, second-order numerical scheme)} \tag{3.56}$$

with

$$\tilde{\mathbf{M}}^B = \mathbf{M}^B \text{ lumped mass matrix.} \tag{3.57}$$

In this case, the algorithm of part (2.2) can be generalized immediately to nonlinear behavior because

$$\mathbf{F}^B_{\text{int}_j} = \mathbf{F}^B_{\text{int}_j}\left(\mathbf{U}^B_j\right) = \mathbf{F}^B_{\text{int}_j}\left({}^{\mathrm{p}}\mathbf{U}^B_{j-1}\right). \tag{3.58}$$

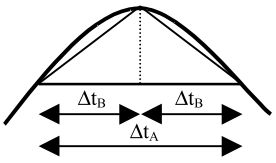

Fig. 2. Energy dissipation in zones where the radius of curvature is small.

Then, Eq. (2.30) is replaced by

$$\mathbf{M}^B \ddot{\mathbf{U}}^B_{j_{sl}} = \mathbf{F}^B_{\mathrm{ext}_j} - \mathbf{F}^B_{\mathrm{int}}\left({}^{\mathrm{p}}\mathbf{U}^B_{j-1}\right) \tag{3.59}$$

and condensation operator (2.26) by

$$\mathbf{H} = \gamma_A m \Delta t \mathbf{C}^A \tilde{\mathbf{M}}^{A^{-1}} \mathbf{C}^{A^{\mathrm{T}}} + \gamma_B \Delta t \mathbf{C}^B \mathbf{M}^{B^{-1}} \mathbf{C}^{B^{\mathrm{T}}}. \tag{3.60}$$

It is important to note that in expression (3.59) the nonlinear term associated with internal forces does not appear in the condensation operator because of the explicit nature of the scheme. Furthermore, the form of the approach chosen accommodates both the implicit linear/explicit nonlinear case and the explicit linear/explicit nonlinear case with large time-steps in the linear subdomain and small time-steps in the explicit nonlinear subdomain. If we consider material nonlinearities only, the shape of the elements does not change throughout the analysis. Hence, the explicit time-step remains constant during the calculation and matrix **H** is constant. When geometric nonlinearities are involved, the explicit time-step may decrease and, in this case, matrix **H** changes. This case will not be not considered in the following discussion.

4. Summary

In Section 2, we proposed two main families of algorithms based on a partition of the domain using a dual Schur formulation. First, in the case of equal time-steps in all subdomains and continuous velocities at the interfaces, we demonstrated the possibility of using different numerical schemes of the Newmark family. Furthermore, we gave the conditions and limitations of doing so in the case of continuous displacements or accelerations at the interfaces. This led us to propose, in the second part, a method with different time-steps in the subdomains, continuous velocities at the interfaces and linear interpolation of velocities. We showed in this case that the stability of the various available schemes is not altered by the decomposition into subdomains or by the linear interpolation of Lagrange multipliers and velocities. However, slight numerical dissipation takes place at the interfaces due to the linear interpolation on the condensed problem. Next, we will verify the announced properties of the method with continuity of velocities at the interfaces and linear interpolation of velocities through numerical examples. For this purpose, we consider the following two cases: implicit linear/explicit linear with different time-steps and implicit linear/explicit nonlinear with different time-steps.

5. Numerical examples

The following examples were calculated using the CASTEM 2000 program developed at *Commissariat à l'Energie Atomique* [24]. In the following discussion, we assume the explicit scheme to be the central difference scheme $\gamma_{\mathrm{E}} = 1/2$ and $\beta_{\mathrm{E}} = 0$ and the implicit numerical scheme to be the mean acceleration scheme $\gamma_{\mathrm{I}} = 1/2$ and $\beta_{\mathrm{I}} = 1/4$. Each example will be compared with two basic solutions obtained with only one subdomain: one using the mean acceleration implicit scheme, and the other using the central difference explicit scheme.

5.1. Case of a structure under bending load

We first consider the case of a cantilever beam with square cross-section subject to a bending load at its extremity. The geometry and material data are the following:

$$L = 4 \text{ m}, \quad E = 210 \times 10^9 \text{ N m}^{-2},$$
$$b = 0.4 \text{ m}, \quad v = 0.3, \tag{5.1}$$
$$S = 0.4 \times 0.4 \text{ m}^2, \quad \rho = 7800 \text{ kg m}^{-3}.$$

In this example, we combine the mean acceleration implicit scheme and the central difference explicit scheme, the material behavior being linear elastic in all subdomains. We divide the structure into four subdomains discretized with 12,076 eight-node cubic finite elements. The number of degrees of freedom equals 9595 (excluding Lagrange multipliers). The mesh of the four subdomains is given in Fig. 3: the green and blue subdomains are chosen to be implicit and the red and yellow subdomains explicit. The interfaces between the different subdomains are chosen to be nonconforming. Furthermore, some interfaces are connected to three or four subdomains. The interfaces are plotted in Fig. 4.

The time-step ratio m between the implicit and explicit subdomains is chosen to be 40:

$$\Delta T = \Delta T_{\text{I}} = 40 \Delta t_{\text{E}}.$$

The leftmost side of the green subdomain is built-in, and the rightmost side of the yellow and blue subdomains is subjected to a transient step load defined in Fig. 5, where $F = 5 \times 10^5$ N and $\tau = 1 \times 10^{-4}$ s. This first example allows us to validate the method in a three-dimensional case. The following curves refer to the displacement and velocity at the end of the bar. The explicit time-step Δt_{E} is defined by the Courant condition [20] calculated on the whole structure. Δt is given by

$$\frac{\Delta t_{\text{I}}}{m} = \Delta t_{\text{E}} = 0.8 \Delta t_{\text{crit}} \approx 5 \times 10^{-6} \text{ s}. \tag{5.2}$$

The analytical maximum dynamic displacement is

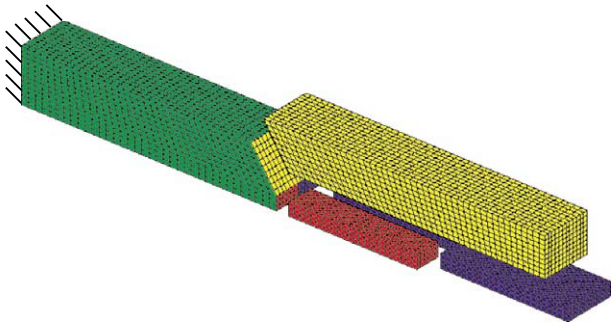

Fig. 3. Mesh of a structure under bending load.

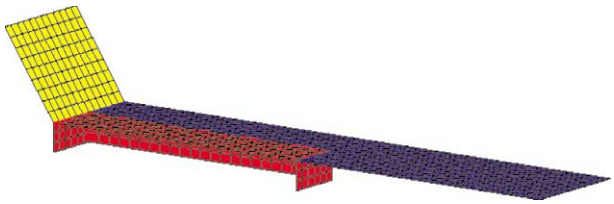

Fig. 4. Representation of the interfaces connected to three or four subdomains.

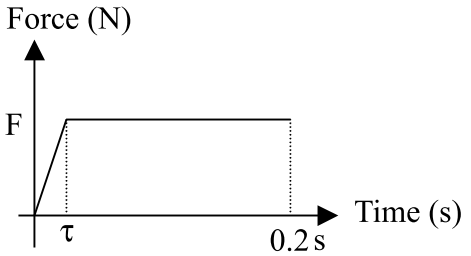

Fig. 5. Structure subjected to a transient step load.

$$w_{\max} = -\frac{8FL^3}{ESb^4} = -4.76 \times 10^{-2} \text{ m}.$$

The number of explicit time-steps equals 40,000 and the number of implicit time-steps equals 1000. Fig. 6 allows us to compare the displacements at the extremity of the beam from the three calculations. The agreement is quite good. In Fig. 7, we show in pink the energy balance for the explicit implicit method, while we can see in red the kinetic energy ΔE_c, in green the work of nonlinear internal forces W_{int} and in blue the work of the external forces W_{ext}. We used the following expression of the discrete energy balance [11] in the linear case, with notations (3.4):

$$\begin{aligned}&\left[T\left(\dot{\mathbf{U}}_n\right)\right] + [V(\mathbf{U}_n)] + \Delta t^2\left(\beta - \tfrac{1}{2}\gamma\right)\left[T\left(\ddot{\mathbf{U}}_n\right)\right] \\ &\quad = -2\left(\gamma - \tfrac{1}{2}\right)V([\mathbf{U}_n]) - \Delta t^2\left(\gamma - \tfrac{1}{2}\right)(2\beta - \gamma)T\left(\left[\ddot{\mathbf{U}}_n\right]\right) + \int_{t_n}^{t_{n+1}} \mathbf{F}_{\text{ext}}^{\text{T}}\dot{\mathbf{U}}\,\mathrm{d}t \end{aligned} \tag{5.3}$$

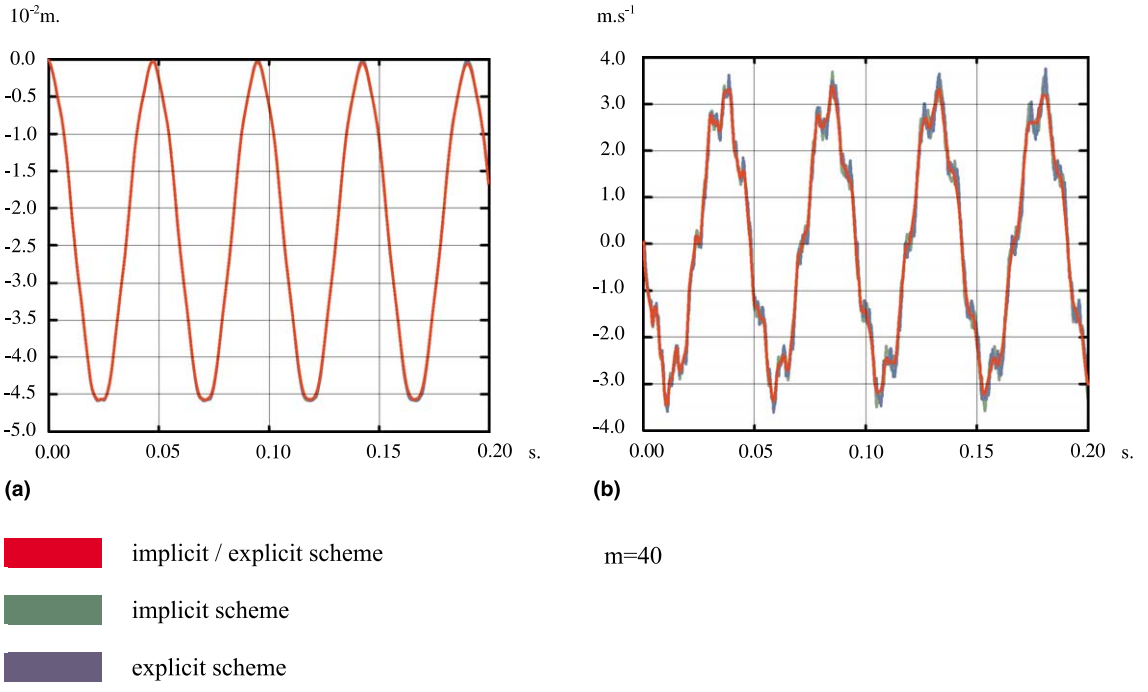

Fig. 6. (a) Vertical displacement at the end of the bar. (b) Vertical velocity at the end of the bar.

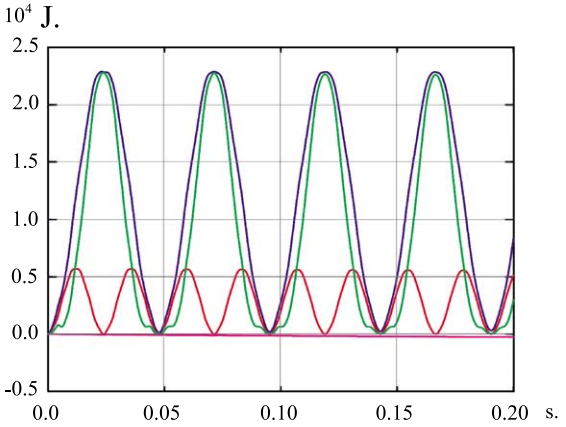

Fig. 7. Energy balance.

and in the nonlinear case

$$\left[T\left(\dot{\mathbf{U}}_n\right)\right] + \Delta t^2\left(\beta - \tfrac{1}{2}\gamma\right)\left[T\left(\ddot{\mathbf{U}}_n\right)\right] = -\Delta t^2\left(\gamma - \tfrac{1}{2}\right)(2\beta - \gamma)T\left(\left[\ddot{\mathbf{U}}_n\right]\right) - \int_{t_n}^{t_{n+1}} \mathbf{F}_{\text{int}}^{\text{T}}\dot{\mathbf{U}}\,\mathrm{d}t + \int_{t_n}^{t_{n+1}} \mathbf{F}_{\text{ext}}^{\text{T}}\dot{\mathbf{U}}\,\mathrm{d}t \tag{5.4}$$

with

$$\int_{t_n}^{t_{n+1}} \mathbf{F}_{\text{ext}}^{\text{T}}\dot{\mathbf{U}}\,\mathrm{d}t = \langle \mathbf{F}_{\text{ext}_n}\rangle^{\text{T}}[\mathbf{U}_n] + \left(\gamma - \tfrac{1}{2}\right)[\mathbf{F}_{\text{ext}_n}]^{\text{T}}[\mathbf{U}_n], \tag{5.5}$$

$$\int_{t_n}^{t_{n+1}} \mathbf{F}_{\text{int}}^{\text{T}}\dot{\mathbf{U}}\,\mathrm{d}t = \langle \mathbf{F}_{\text{int}_n}\rangle^{\text{T}}[\mathbf{U}_n] + \left(\gamma - \tfrac{1}{2}\right)[\mathbf{F}_{\text{int}_n}]^{\text{T}}[\mathbf{U}_n]. \tag{5.6}$$

Remark.

- From (5.3), if, $\gamma = \frac{1}{2}$, $\beta = \frac{1}{4}$ and $\mathbf{F}_{\text{ext}} = 0$, then $[T(\dot{\mathbf{U}}_n)] + [V(\mathbf{U}_n)] = 0$. In other terms, the total energy is preserved.
- From (5.3), if $\gamma = \frac{1}{2}$ and $\mathbf{F}_{\text{ext}} = 0$, then $[T(\dot{\mathbf{U}}_n)] + [V(\mathbf{U}_n)] + \Delta t^2(\beta - \frac{1}{2}\gamma)[T(\ddot{\mathbf{U}}_n)]$ is preserved.
- If we consider the subdomains, we can use expressions (5.3) or (5.4) on each subdomain with its own timescale. Furthermore, the global discrete energy balance enables us to evaluate the interface work or, in other words, the dissipation at the interfaces using the following equation:

$$W_{\text{interface}} = \Delta E_c^A + \Delta E_c^B - W_{\text{ext}}^A - W_{\text{ext}}^B + W_{\text{int}}^A + W_{\text{int}}^B. \tag{5.7}$$

With this example, we can make the following remarks: on the one hand, the method lends itself to any interface geometry, provided that we define the link conditions at the interfaces correctly using, for instance, the technique explained in [25]. On the other hand, the phase and amplitude of the displacements and velocities are not affected by the decomposition into subdomains. The numerical

dissipation related to the interpolation of velocities and to the different time-steps appears to be small when $m = 40$.

5.2. Case of a clamped axisymmetric plate under bending load

In this example, we consider a circular plate clamped on its periphery and subjected to a bending load at its center. In this example, we combine the mean acceleration implicit scheme with linear elastic properties and the central difference explicit scheme with nonlinear material behavior in the subdomain subject to the load. We divide the structure into three subdomains discretized with 864 quadrilateral and triangular axisymmetric finite elements. The total number of degrees of freedom equals 965 (excluding Lagrange multipliers). The time-step ratio m chosen is 100.

The green subdomain in Fig. 8 is chosen to be implicit while the blue subdomains are nonlinear explicit. The mesh is refined towards the center of the plate where failure is expected. The characteristics of the structure are similar for all subdomains and defined by

$$\begin{aligned} &R = 1 \text{ m}, \quad \text{radius}, \\ &e = 0.1 \text{ m}, \quad \text{thickness}, \\ &E = 210 \times 10^9 \text{ Pa}, \quad \text{Young's modulus}, \\ &v = 0.3, \quad \text{Poisson parameter}, \\ &\rho = 7800 \text{ kg m}^{-3}, \quad \text{density}. \end{aligned} \tag{5.8}$$

In the implicit subdomain, we assume linear elastic material behavior, whereas in the explicit subdomains the material is elastic–plastic with linear kinematic strain hardening. The initial yield stress and strain hardening parameters are defined by

$$\begin{aligned} &\sigma_Y = 400 \times 10^6 \text{ Pa}, \\ &h = E/1000. \end{aligned} \tag{5.9}$$

The right edge of the model is clamped, and the top part of the left subdomain is subjected to a transient vertical load F described in Fig. 9, where $F = 1 \times 10^6$ N and $\tau = 1 \times 10^{-4}$ s. This second example allows us

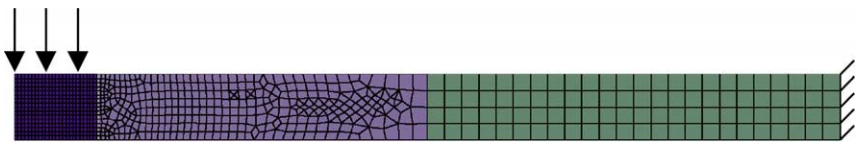

Fig. 8. Representation of the mesh of the plate with a refined mesh towards the center.

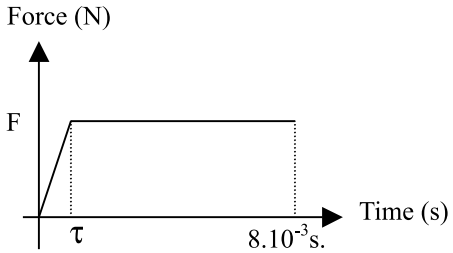

Fig. 9. Structure subjected to a transient step load.

to evaluate the interest of the method in a case where there are localized nonlinear zones. The time-step is defined by the Courant condition [20] calculated on the whole structure:

$$\frac{\Delta t_{\mathrm{I}}}{m} = \Delta t_{\mathrm{E}} = 0.8\Delta t_{\mathrm{crit}} \approx 1.6 \times 10^{-7} \text{ s.} \tag{5.10}$$

The number of explicit time-steps is 40,000 and the number of implicit time-steps equals 400. The various curves presented here are related to the displacement and velocity at the center of the plate. Here, again, we compare in Figs. 10(a) and (b) the solutions obtained with the three approaches: one subdomain (explicit), one subdomain (implicit) and three subdomains (explicit and implicit).

We observe very good agreement for displacements and velocities. At the final time $t = 6 \times 10^{-3}$ s, the deformed structure (amplified 10 times) has the shape given in Figs. 11(a)–(c). Fig. 11(a) (resp. 13(b) and (c)) shows the ε_{rr} (resp. ε_{zz}, γ_{rz}) isostrains.

In Fig. 11(d), we compare the radial strains ε_{rr} at the center of the plate given by the three methods considered. In Fig. 11(e), we plotted the energy balance for the coupled algorithm. The red curve represents the Kinetic energy, the blue curve the work of external loads, the green curve the work of internal loads and the pink curve the work at the interfaces (which should be zero). We can observe that this work is indeed very small – the maximum value is 1.2 against a typical order of magnitude of 10^4 J. The ratio of the maximum energy dissipated at the interfaces to the maximum work of external loads is about 10^{-5}. Finally, in this example, we can make remarks similar to those of the first example: on the one hand, the responses in terms of displacement, velocity and localized strain are very close for all schemes, hence the numerical dissipation and dispersion seem to be very small. On the other hand, the numerical dissipation effect due to the numerical scheme appears to be small and, therefore, acceptable for a time-step ratio $m = 100$ between explicit and implicit schemes and with nonlinear material behavior in the explicit subdomains.

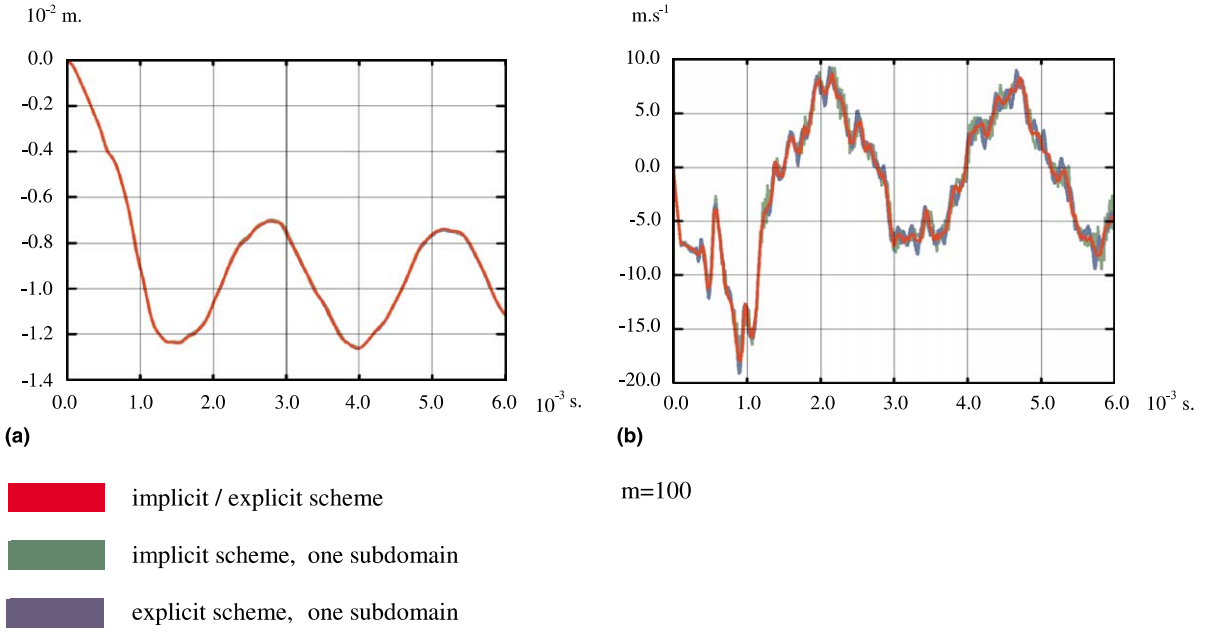

Fig. 10. (a) Vertical displacement at center of the plate. (b) Vertical velocity at center of the plate.

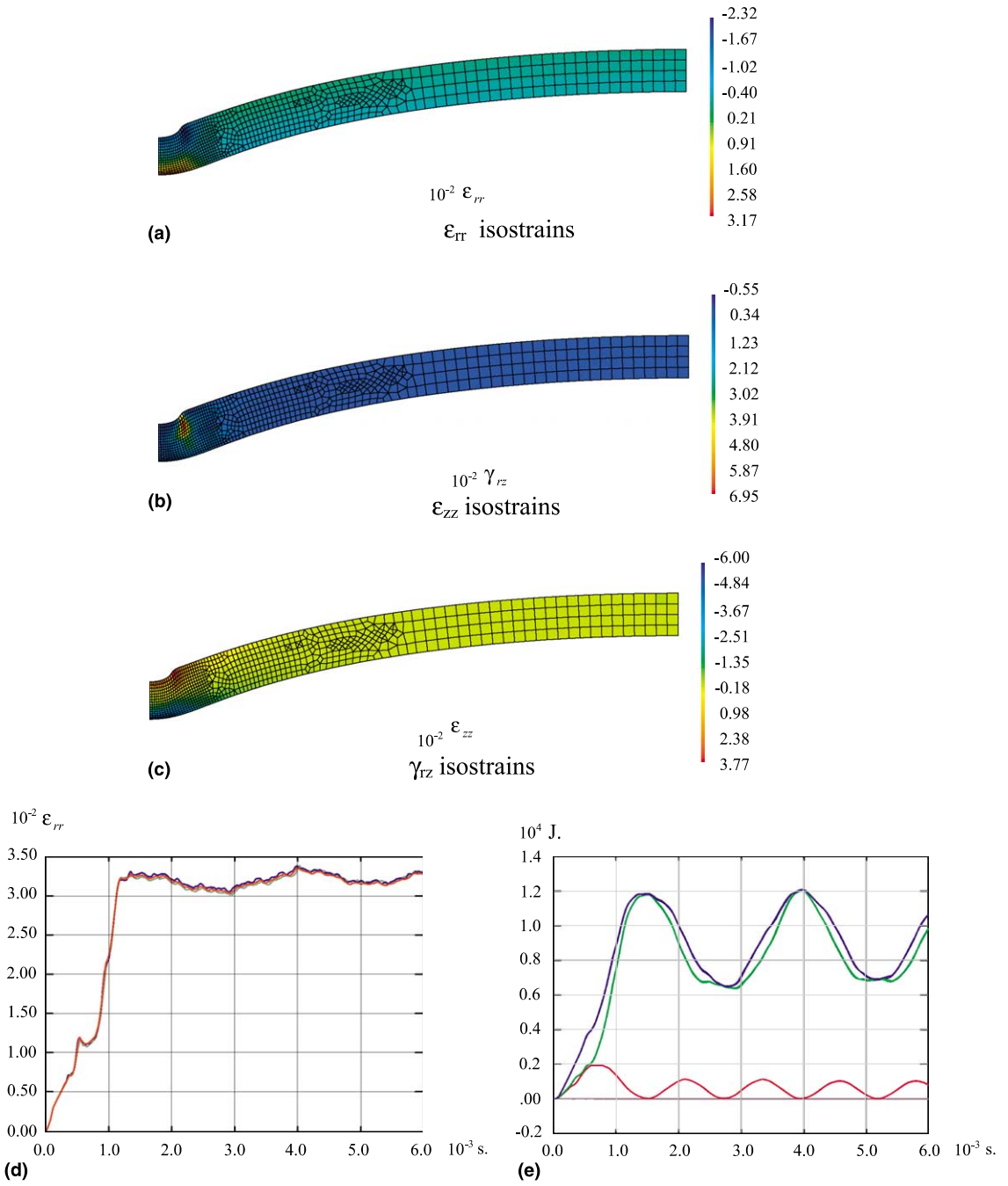

Fig. 11. (a) ε_{rr} isostrains. (b) ε_{zz} isostrains. (c) γ_{rz} isostrains. (d) Deformation at the center of the plate. (e) Energy balance.

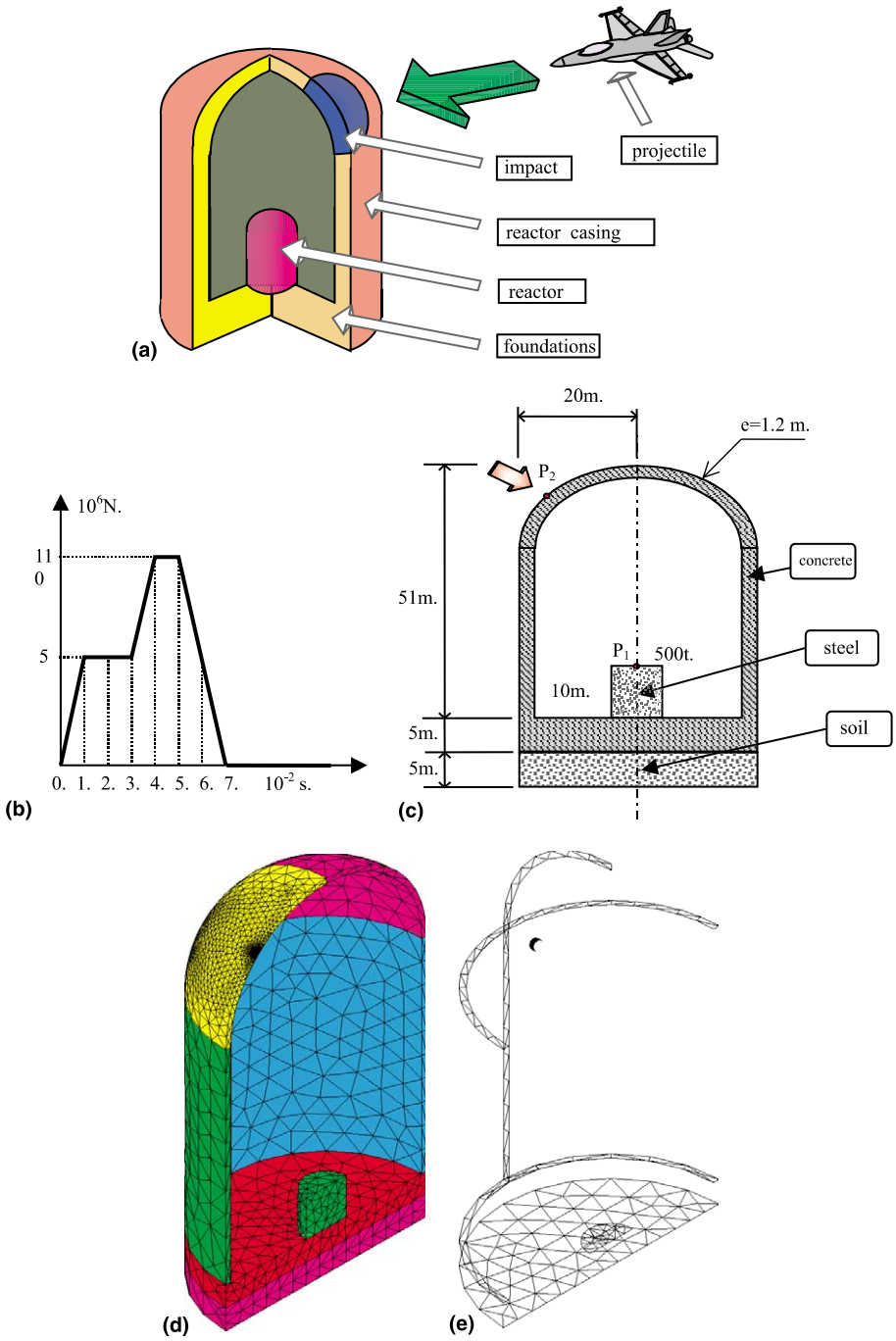

Fig. 12. (a) Case of an impact on the containment vessel of a nuclear reactor casing. (b) Normal load applied at the point of impact. (c) Geometry of the structure. (d) Mesh of the structure. (e) Mesh of the interfaces.

5.3. Case of an impact on the containment vessel of a nuclear reactor casing

We will now study a simplified model of a nuclear reactor containment vessel and the effect of an impact on the structure using a subdomain dynamic method (see Fig. 12).

The objective is to calculate the short-term (perforation) and mid-term (shaking) consequences of such an impact [15,26]. Accordingly, we consider an explicit calculation at impact level ($t \leqslant 0.1$ s) and an implicit calculation for the rest of the structure (vibration phenomena with durations on the order of a second). The normal loads applied at the point of impact and the geometry of the structure are defined in Figs. 12(b) and (c). We model the structure using tetrahedral finite elements in each subdomain. We partition the domain

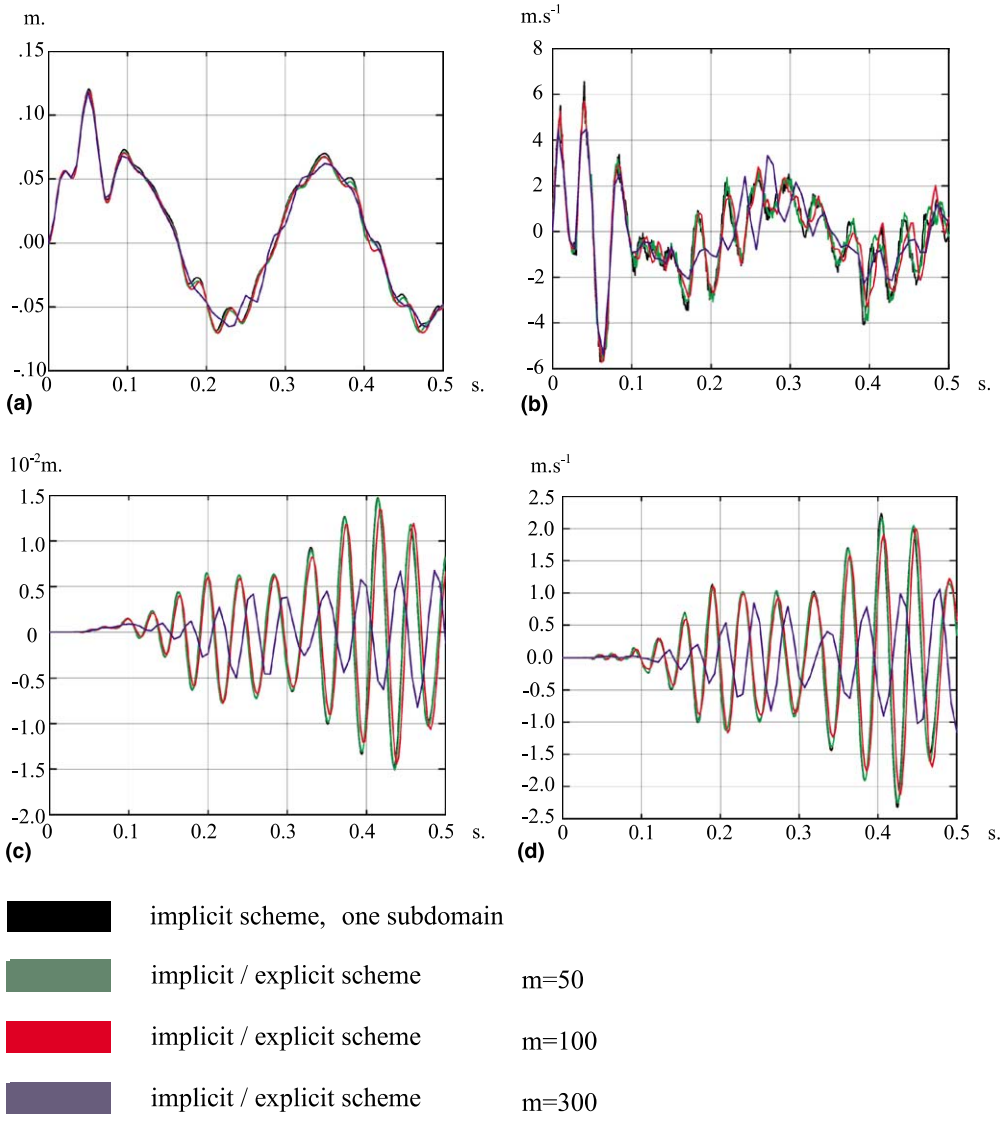

Fig. 13. (a) Horizontal displacement at P_2. (b) Horizontal velocity at P_2. (c) Horizontal displacement at P_1. (d) Horizontal velocity at P_1.

into eight subdomains with the following characteristics: the subdomain corresponding to the impact is calculated with the central difference numerical scheme and nonlinear elastic–plastic material behavior of the Prager type (tensile limit: $0.3\sigma_m$; compression limit: $3\sigma_m$; with $\sigma_m = 400 \times 10^6$ Pa); the adjacent subdomain is also explicit, but with linear elastic material behavior; the remaining six subdomains are calculated using the mean acceleration numeric scheme and a linear elastic material. In this calculation, we consider three ratios of time-steps between the explicit and the implicit cases, namely 50, 100 and 300. The impact is represented by a distributed load on the surface of the explicit subdomain. The reactor casing is coarsely represented by a 500-ton added mass at point P_1. The characteristics of the outer shell, soil and casing are the following:

$$\text{Soil} \quad \begin{cases} \rho_A = 3000 \text{ kg m}^{-3}, \\ E_A = 0.1 \times 10^{11} \text{ N m}^{-2}, \\ \nu = 0.3, \end{cases} \tag{5.11}$$

$$\text{Shell} \quad \begin{cases} \rho_A = 2500 \text{ kg m}^{-3}, \\ E_A = 0.419 \times 10^{11} \text{ N m}^{-2}, \\ \nu = 0.2, \end{cases} \tag{5.12}$$

$$\text{Casing} \quad \begin{cases} \rho_A = 7800 \text{ kg m}^{-3}, \\ E_A = 210 \times 10^{9} \text{ N m}^{-2}, \\ \nu = 0.3. \end{cases} \tag{5.13}$$

The explicit time-step is

$$\Delta t_E = 7.35 \times 10^{-6} \text{ s}. \tag{5.14}$$

In this model, we prescribe continuous velocities at the interfaces. Figs. 12(d) and (e) show the mesh of the structure partitioned into eight subdomains and the mesh of the interfaces between the subdomains. One can see that the mesh size of the impacted subdomain is much finer than that of the implicit subdomains in the shell and that of the interfaces, which are coarsely meshed (see Figs. 12(d) and (e)).

The mesh has 6955 elements and 7710 degrees of freedom. Figs. 13(a) and (b) (resp. 13(c) and (d)) represent the horizontal displacement and horizontal velocity of node P_2 (resp. P_1) for the time interval considered, i.e. 0.5 s. The three cases of time-step ratios considered are compared with the results of a numerical calculation performed with the same constitutive equations, but using a mean acceleration implicit Newton–Raphson iterative algorithm without domain decomposition.

The results obtained agree with the theoretical results for stability obtained in Section 3: continuous velocities at the interface with interpolated velocities allow time-step ratios of about 100 with no degradation of the solution (reference calculation black line, $m = 50$ green line, $m = 100$ red line, $m = 300$ blue line). For a time-step ratio of 300, the long-term solution is damped and the phase is altered. It is clear, in this case, that dissipation at the interfaces is high. Furthermore, it seems that a large number of interfaces causes more energy to be dissipated at the interface. This is an important parameter, and a criterion for the choice of the maximum allowable ratio of time-steps between subdomains remains to be formulated. Some more work is necessary in order to be able to control the conditions for time-step ratio a priori, as well as to decrease the number of interfaces.

6. Conclusions

We proposed a new method of coupling subdomains with arbitrary Newmark numerical schemes within the framework of a dual Schur formulation. We also showed that, in the case of continuous velocities at the

interfaces with linear velocity interpolation, the decomposition into subdomains does not alter the stability of the numerical schemes in each subdomain. This enabled us to demonstrate the validity of the method in the case of coupling between implicit linear/explicit material nonlinear numerical schemes with a time-step ratio on the order of 100. The validation on three three-dimensional examples with linear and nonlinear material behavior in the explicit subdomains allows us to consider expanding the method to other cases which could benefit from the formulation using Lagrange multipliers [27–29], particularly in the case of incompatible meshes at the interfaces, or in the case of impact problems, of for multi-physics problems. Finally, the mid-term perspectives are the extension of nonlinear behavior to the implicit subdomains, the extension to large displacements, and developments to take advantage of the suitability of the algorithm for parallel computations.

Acknowledgements

We wish to thank the reviewer for his suggestions, which helped improve the paper.

References

[1] A. de Gayffier, Y. Nuttinck, Une méthode de décomposition de domaine par multiplicateurs de lagrange pour la dynamique des structures, CEA, Rapport interne, 1997.
[2] A. de Gayffier, C. Duval, A review of rheological concrete models for aircraft impact problems in nuclear power plants, in: SMIRT 14, Lyon, France, August 1997.
[3] A. Combescure, A. de Gayffier, A. Gravouil, N. Greffet, A Lagrange multiplier based domain decomposition method for time-dependent problems involving several timescales, in: IV World Congress on Computational Mechanics, 1998.
[4] Y.H. De Roeck, P. Le Tallec, M. Vidrascu, A domain decomposed solver for nonlinear elasticity, Comput. Methods Appl. Mech. Engrg. 99 (1992) 187–207.
[5] S. Meynen, Domain decomposition methods for the solution of non-linear problems in solid mechanics, in: Advances in Computational Mechanics with High Performance Computing, Civil-Comp. Press, Edinburgh, 1998, pp. 87–94.
[6] C. Farhat, Roux, Implicit parallel processing in structural mechanics, Comput. Mech. Adv. (2) (1994).
[7] W.K. Liu, T. Belytshko, Mixed-time implicit–explicit finite elements for transient analysis, Comput. Struct. 15 (1982) 445–450.
[8] T. Belytschko, B.E. Engelmann, W.K. Liu, A Review of Recent Developments in Time Integration, The American Society of Mechanical Engineers, 1989, pp. 185–199.
[9] I. Miranda, R.M. Ferencz, T.J.R. Hughes, An improved implicit–explicit time integration method for structural dynamics, Earthquake Engrg. Struct. Dynamics 18 (1989) 643–653.
[10] E.D. Sotelino, A concurrent explicit–implicit algorithm in structural dynamics, Comput. Struct. 51 (2) (1994) 181–190.
[11] T.J.R. Hughes, T. Belytschko, Nonlinear finite element analysis, ICE Division, Zace Services Ltd., 1995.
[12] M. Fortin, R. Glowinski, Les Méthodes de Lagrangien Augmenté, Dunod, Paris, 1982.
[13] P.L. Lions, On the Schwarz alternating method, in: Chan, Glowinski, Périaux, O. Windlun (Eds.), Proceedings of Domain Decomposition Methods for Partial Differential Equations, SIAM, Philadelphia, PA, 1990.
[14] F.X. Roux, Méthodes de résolution par sous-domaines en statique, La Recherche Aérospatiale (1) (1990) 37–48.
[15] J. Bonini, H. Bung, Modélisation des problèmes de contact-impact avec frottement en explicite par la méthode des multiplicateurs de Lagrange, 3ème Colloque National en Calcul des Structures, Giens, 1997, pp. 411–416.
[16] C. Farhat, C. Mandel, A scalable Lagrange multiplier based domain decomposition method for time-dependent problems, Int. J. Numer. Methods Engrg. (38) (1995) 3831–3853.
[17] M.N. Newmark, A method of computation for structural dynamics, in: Proceedings of ASCE 85, EM3, 1959.
[18] O.C. Zienkiewicz, A new look at the Newmark, Houbolt and other time stepping formulas. A weighted residual approach, Earthquake Engrg. Struct. Dynamics 5 (1977) 413–418.
[19] A. de Gayffier, M. Lepareux, H. Bung, A. Letellier, Réflexions sur les méthodes de la dynamique explicite dans CASTEM 2000 et PLEXUS, Rapport interne CEA, 1996.
[20] A. de Gayffier, H. Bung, J. Bonini, M. Lepareux, Dynamique explicite dans CASTEM 2000. Spécifications et développements, Rapport interne CEA, 1997.
[21] C. Farhat, L. Crivelli, M. Géradin, On the spectral stability of time integration algorithms for a class of constrained dynamics problems, in: AIAA 34th Structural Dynamics Meeting, 1993.

[22] M. Géradin, D. Rixen, Théorie des Vibrations. Application à la Dynamique des Structures, Masson, Paris, 1993.
[23] P. Pegon, On a new characterization of the performance of time integration schemes: application to the α-method scheme, in: 14th SMIRT Conference, Lyon, 1997, Paper B02/3.
[24] P. Verpeaux, T. Charras, A. Millard, CASTEM 2000 une approche moderne du calcul des structures, in: J.M. Fouet, P. Ladevèze, R. Ohayon (Eds.), Calcul des Structures et Intelligence Artificielle, Pluralis, 1988, pp. 261–271.
[25] C. Farhat, J. Mandel, F.X. Roux, Optimal convergence properties of the FETI domain decomposition method, Comput. Methods Appl. Mech. Engrg. 115 (1994) 365–385.
[26] R.L. Taylor, P. Papadopoulos, On a finite element method for dynamic contact/impact problems, Int. J. Numer. Methods Engrg. 36 (1993) 2123–2140.
[27] T. Sassi, Méthodes de décomposition de domaines pour la résolution de problèmes d'élasticité non-linéaire avec maillages incompatibles, Thèse de doctorat, Université Paris IX, Dauphine, 1993.
[28] D. Dureisseix, P. Ladevèze, Parallel and multi-level strategies for structural analysis, Actes du Colloque ECCOMAS, Paris, 1996.
[29] D. Dureisseix, Une approche multi-échelles pour des calculs de structures sur ordinateurs à architecture parallèle, Laboratoire de Mécanique et Technologie/ENS de CACHAN/CNRS/Université Paris 6, France, Thèse de doctorat, 1997.